3

Direct Torque Control using Space Vector Modulation and Dynamic Performance of the Drive, via a Fuzzy Logic Controller for Speed Regulation

Adamidis Georgios, and Zisis Koutsogiannis
Democritus University of Thrace
Greece

1. Introduction

During the last decade, a lot of modifications in classic Direct Torque Control scheme (Takahashi & Noguchi, 1986) have been made (Casadei et al., 2000), (Reddy et al., 2006), (Chen et al., 2005), (Grabowski et al., 2005), (Romeral et al., 2003), (Ortega et al., 2005). The objective of these modifications was to improve the start up of the motor, the operation in overload conditions and low speed region. The modifications also aimed to reduce the torque and current ripple, the noise level and to avoid the variable switching frequency by using switching methods with constant switching frequency.
The basic disadvantages of DTC scheme using hysteresis controllers are the variable switching frequency, the current and torque ripple. The movement of stator flux vector during the changes of cyclic sectors is responsible for creating notable edge oscillations of electromagnetic torque. Another great issue is the implementation of hysteresis controllers which requires a high sampling frequency. When an hysteresis controller is implemented using a digital signal processor (DSP) its operation is quite different to the analogue one.
In the analogue operation the value of the electromagnetic torque and the magnitude of the stator flux are limited in the exact desirable hysteresis band. That means, the inverter can change state each time the torque or the flux magnitude are throwing the specified limits. On the other way, the digital implementation uses specific sample time on which the magnitudes of torque and flux are checked to be in the desirable limits. That means, very often, torque and flux can be out of the desirable limits until the next sampling period. For this reason, an undesirable torque and flux ripple is occurred.
Many researchers are oriented to combine the principles of DTC with a constant switching frequency method for driving the inverter by using space vector modulation. This requires the calculation in the control schemes of the reference voltage vector which must be modulated in the inverter output. Therefore, the Direct Torque Control with Space Vector Modulation method (DTC-SVM) is applied (Koutsogiannis & Adamidis 2007). Since we know the reference voltage vector it is easy to perform the modulation by applying specific switching pattern to the inverter (Koutsogiannis & Adamidis 2006). In the DTC scheme a speed estimation and a torque control are applied using fuzzy logic (Koutsogiannis & Adamidis 2006). An improvement of DTC with a parallel control FOC is observed (Casadei

et al., 2002). The use of the rotor flux magnitude instead of the stator flux magnitude, improves the overload ability of the motor. This control is sensitive to the machine's parameters during transient operations.
Also, the DTC-SVM can be applied using closed loop torque control, for minimization of torque ripple (Wei et. al., 2004). In this case estimation of stator and rotor flux is required. Therefore, all the parameters of the induction motor must be known (Reddy et al., 2006). A new method was developed that allows sensorless field-oriented control of machines with multiple non-separable or single saliencies without the introduction of an additional sensor (Zatocil, 2008). In this paper, the closed loop torque control method is applied which improves the torque response during dynamic and steady state performance. A lot of papers for the speed control of electrical drives, which uses different strategies based on artificial intelligence like neural network and fuzzy logic controller, have presented. For the fuzzy PI speed controller its robustness and disturbance rejection ability Gadou et. Al., 2009) is demonstrated. In this paper fuzzy logic for the speed estimation of the motor and the method DTC-SVM with closed loop torque control will be applied. This paper is further extended through a further improvement of the system control by controlling the magnitudes of torque and flux using closed loop control. The simulation results were validated by experimental results.

2. Overview of the classic DTC scheme

The classic DTC scheme is shown in figure 1.

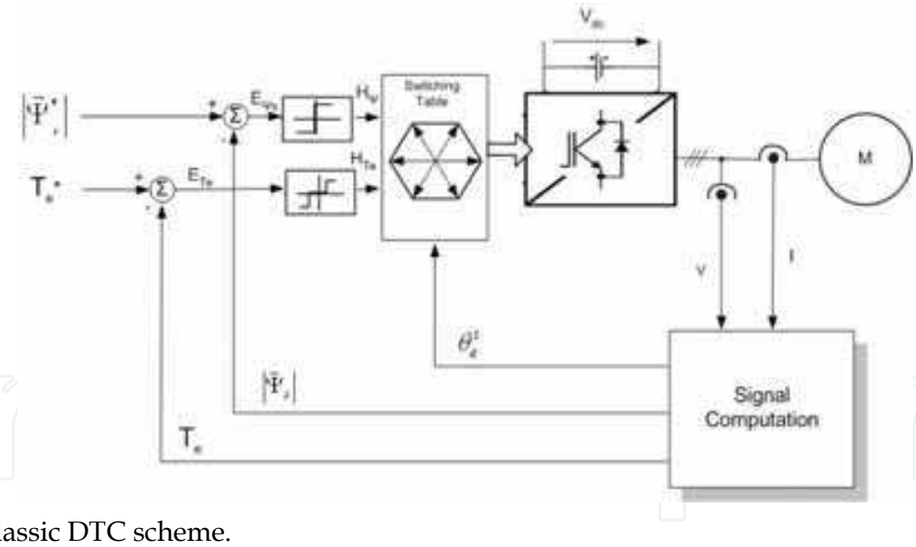

Fig. 1. Classic DTC scheme.

DTC based drives require only the knowledge of the stator resistance R_s. Measuring the stator voltage and current, stator flux vector can be estimated by the following equation:

$$\vec{\psi}_s = \int \left(\vec{V}_s - R_s \vec{I}_s \right) dt \tag{1}$$

the stator flux magnitude is given by,

$$\left| \vec{\Psi}_s \right| = \sqrt{\Psi_{as}^2 + \Psi_{\beta s}^2} \tag{2}$$

where the indicators *a,β* indicates the *a-β* stationary reference frame. The stator flux angle is given by,

$$\theta_e = \sin^{-1}\frac{\Psi_{\beta s}}{\left|\vec{\Psi}_s\right|} \tag{3}$$

and the electromagnetic torque T_e is calculated by,

$$T_e = \frac{3}{2}\left(\frac{P}{2}\right)\left(\Psi_{\alpha s} i_{\beta s} - \Psi_{\beta s} i_{\alpha s}\right) \tag{4}$$

where P is the number of machine poles.

In the DTC scheme the electromagnetic torque and stator flux error signals are delivered to two hysteresis controllers as shown in figure 1. The stator flux controller imposes the time duration of the active voltage vectors, which move the stator flux along the reference trajectory, and the torque controller determinates the time duration of the zero voltage vectors, which keep the motor torque in the defined-by-hysteresis tolerance band. The corresponding output variables H_{Te}, H_Ψ and the stator flux position sector $\theta_{\Psi s}$ are used to select the appropriate voltage vector from a switching table scheme (Takahashi & Noguchi, 1986), which generates pulses to control the power switches in the inverter. At every sampling time the voltage vector selection block chooses the inverter switching state, which reduces the instantaneous flux and torque errors.

In practice the hysteresis controllers are digitally implemented. This means that they function within discrete time Ts. Consequently, the control of whether the torque or the flux is within the tolerance limits, often delays depending on the duration of the sampling period. This results in large ripples in the torque and the current of the motor. In conclusion, the abrupt and undesirable ripples in the electromagnetic quantities appear when the control of the values of the torque and the flux takes place at times when their values are near the allowed limits. This means that a voltage vector will be chosen which will continue to modify these quantities in a time Ts, even though these limits have been practically achieved. Accordingly, in the next control which will be carried out after time Ts, these quantities will be quite different from the desirable values. Another reason why the electromagnetic torque of the motor presents undesirable ripples is the position of the $\vec{\psi}_s$ in each of the six sectors of its transition. In general, an undesired ripple of the torque is observed when the $\vec{\psi}_s$ moves towards the limits of the cyclic sectors and generally during the sectors' change. Furthermore, the torque ripple does not depend solely on the systems conditions but on the position of $\vec{\psi}_s$ in the sector as well. Therefore, we can establish that there are more control parameters which could affect the result of the motor's behavior.

3. DTC-SVM with closed-loop torque control

In this section, the DTC-SVM scheme will be presented which uses a closed loop torque control. The block diagram of this scheme is shown in figure 2.

The objective of the DTC-SVM scheme, and the main difference between the classic DTC, is to estimate a reference stator voltage vector V^*_S in order to drive the power gates of the inerter with a constant switching frequency. Although, the basic principle of the DTC is that the electromagnetic torque of the motor can be adjusted by controlling the angle δ_Ψ between

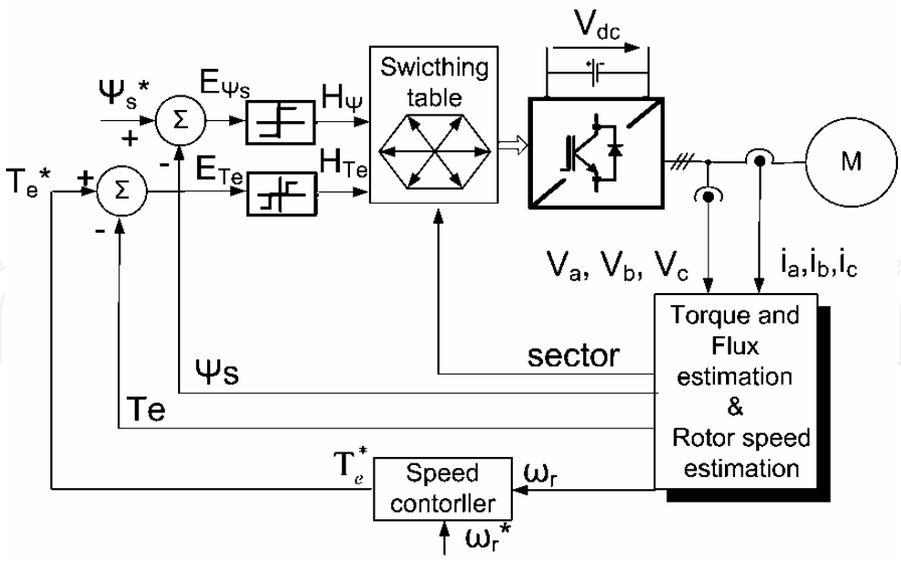

Fig. 2. DTC-SVM with closed-loop torque control

the stator and rotor magnetic flux vectors. Generally, the torque of an asynchronous motor can be calculated by the following equation.

$$T_e = \frac{3}{2}\left(\frac{P}{2}\right)\frac{L_m}{L_r L_s^{'}}\left|\Psi_r\right|\left|\Psi_s\right|\sin\delta_\psi \tag{5}$$

Where $L_s^{'} = L_s L_r - L_m^2$. The change in torque can be given by the following formula,

$$\Delta T_e = \frac{3}{2}\left(\frac{P}{2}\right)\frac{L_m}{L_r L_s^{'}}\left|\Psi_r\right|\left|\vec{\Psi}_s + \Delta\vec{\Psi}_s\right|\sin\Delta\delta_\psi \tag{6}$$

where the change in the stator flux vector, if we neglect the voltage drop in the stator resistance, can be given by the following equation,

$$\Delta\vec{\Psi}_s = \vec{V}_s \Delta t \tag{7}$$

where $\Delta t = Ts$, is the sampling period.

Generally, the classic DTC employs a specific switching pattern by using a standard switching table. That means the changes in the stator flux vector and consequently the changes in torque would be quite standard because of the discrete states of the inverter. That happens because the inverter produces standard voltage vectors.

The objective of the DTC-SVM scheme, and the main difference between the classic DTC, is to estimate a reference stator voltage vector V^*_S and modulate it by SVM technique, in order to drive the power gates of the inerter with a constant switching frequency. Now, in every sampling time, inverter can produce a voltage vector of any direction and magnitude. That means the changes in stator flux would be of any direction and magnitude and consequently the changes in torque would be smoother.

According to above observations, and bearing in mind figure 2, we can see that torque controller produces a desirable change in angle $\Delta\delta_\Psi$ between stator and rotor flux vectors.

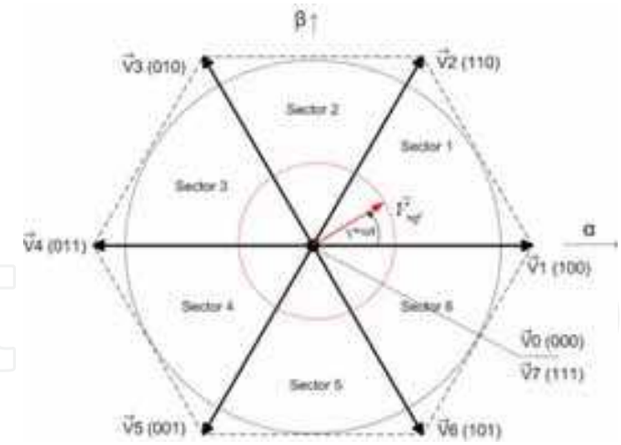

(a)

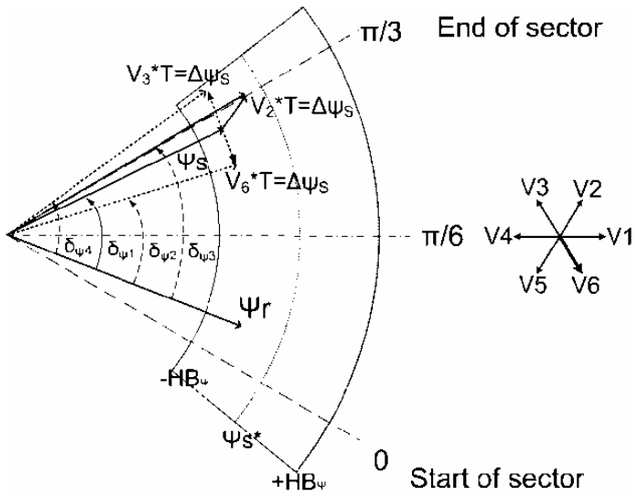

(b)

Fig. 3. Principle of Space Vector Modulation (SVPWM)
(a)reference stator vector
(b) modulation of space vector during one switching period which is equal to sampling time of the DTC-SVM method.

The change in angle $\Delta\delta_\psi$ is added in the actual angle of stator flux vector, so we can estimate the reference stator flux vector by using the following formula, in stationary reference frame.

$$\vec{\psi}_s^* = \left|\vec{\psi}_s^*\right| e^{j\left(\omega_e t + \Delta\delta_\psi\right)} \tag{8}$$

Applying a phasor abstraction between the reference and the actual stator flux vector we can estimate the desirable change in stator flux $\Delta\Psi_S$. Having the desirable change in stator flux, it is easy to estimate the reference stator voltage vector:

$$\vec{V}_s^* = \frac{\Delta\vec{\Psi}_s}{T_S} + R_s\vec{I}_s \tag{9}$$

If the reference stator voltage vector is available, it is easy to drive the inverter by using the SV-PWM technique. So, it is possible to produce any stator voltage space vector (figure 3). As it mentioned before, in the classic DTC scheme, the direction of stator flux vector changes $\Delta\vec{\psi}_S$ are discrete and are almost in the same direction with the discrete state vectors of the inverter. Consequently, in DTC-SVM, stator flux vector changes $\Delta\vec{\psi}_S$ can be of any direction, which means the oscillations of $\vec{\psi}_S$ would be more smoother.

4. Simulation results of DTC and DTC-SVM

The DTC schemes, that are presented so far, are designed and simulated using Matlab/Simulink (figure 4). The proposed scheme is simulated and compared to the classic one. The dynamic and also the steady state behavior is examined in a wide range of motor speed and operating points.

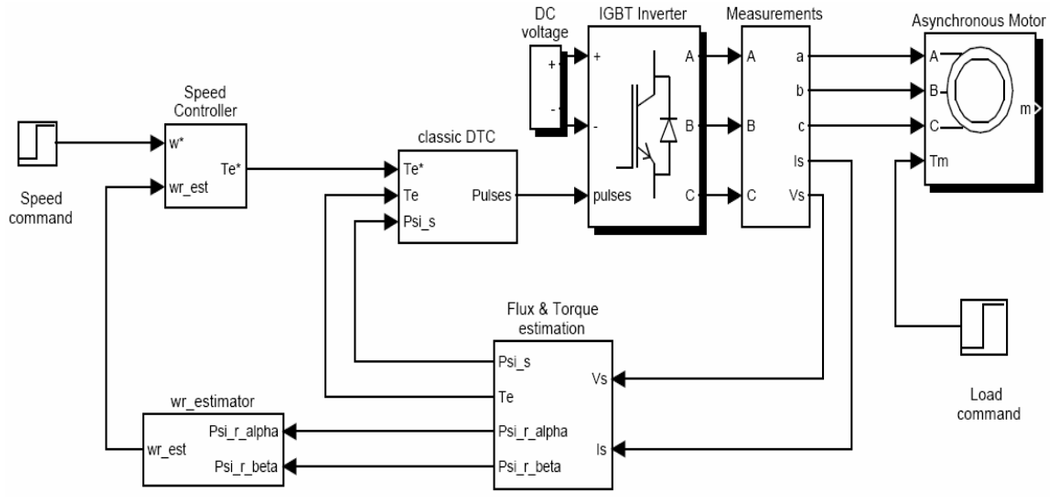

(a)

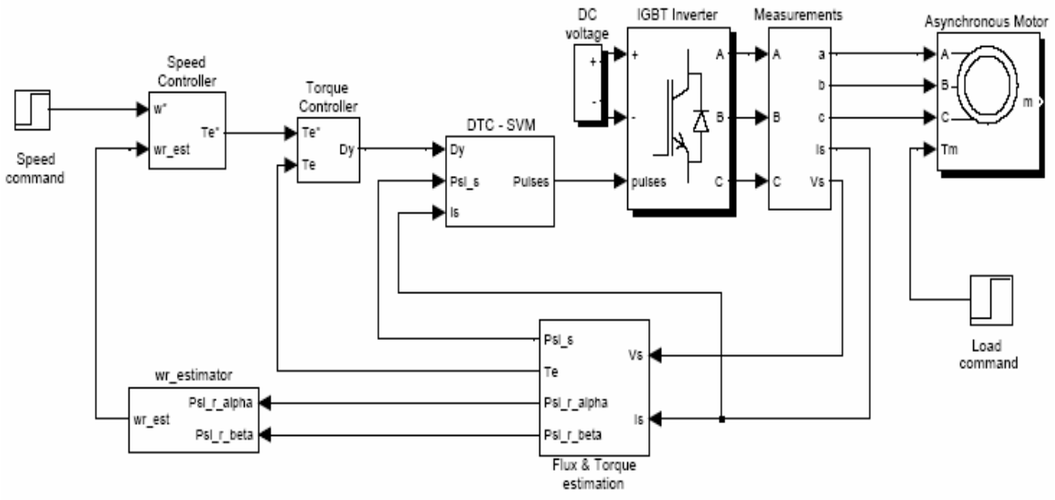

(b)

Fig. 4. Simulink models of (a) classic DTC and (b) DTC-SVM.

For simulation purposes, an asynchronous motor is used and its datasheets are shown in the following table I. The nominal values of the asynchronous motor in the simulation system are the same with the nominal values of the asynchronous motor in the experimental electrical system.

P = 4 (2 pair of poles), f = 50 Hz	R_s = 2,81 Ω	L_s = 8,4 mH
230V/ 400V	R'_r = 2,78 Ω	L'_r = 8,4 mH
P = 2,2 kW, N_r = 1420 rpm	L_m = 222,6 mH	
J = 0.0131 kgm²		

Table I. Nominal values of motor.

For the simulations a particular sampling period T_{S_DTC} for torque and flux was chosen as well as the proper limits HB_{ψ} and HB_{Te} for the hysteresis controllers, in order to achieve an average switching frequency which shall be the same with the constant switching frequency produced by the DTC-SVM control. During the simulation, the dynamic behavior of the system has been studied using both the DTC and the DTC-SVM method.

4.1 Steady state operation of the system

The results of the simulations are presented in the figure 5, where the electromechanical magnitudes of the drive system are shown, for both control schemes in various operation points. In more detail, in figure 5 the operation of the system for low speed and low load is shown and figure 6 shows the motor operation in normal mode. All the electromechanical quantities are referred to one electrical period based on the output frequency of the inverter. The average number of switching for the semiconducting components of the inverter during the classic DTC is almost the same with the number of switching of the DTC-SVM method where the switching frequency is constant. In fact, for the classic DTC flux variation of the hysteresis band equal to HB_{Ψ}=0.015 was chosen, which is almost 2% of the nominal flux and for the torque the hysteresis band controller was chosen to be HB_{Te}=0,65, which means 3% of the nominal torque. These adjustments led to an average switching number of inverter states equal to 17540 per second, for the classic DTC, while for the DTC-SVM a switching frequency equal to 2.5kHz was chosen, namely 15000 switching states per second.

The classic DTC has some disadvantages, mainly in the low speed region with low mechanical load in the shaft, where the current ripple is very high, compared to DTC-SVM (figure 5). Also, the classic DTC has variable switching frequency, where it is observed that the switching frequency is high in low speed area and low in high speeds. In practice, it is not easy to change the sampling period of the hysteresis controllers with respect to the operation point of the drive system. For this reason, a value of the sampling period is chosen from the beginning, which shall satisfy the system operation in the complete speed range. The high ripple observed in the classic DTC electrical magnitudes during the operation in low speed area, is due to the fact that many times, instead of choosing the zero voltage vector for the inverter state, in order to reduce the torque, the backwards voltage vector is chosen, which changes the torque value more rapidly.

Figure 6 shows the motor operation in normal mode. The switching frequency is also at the same value in order to have a right comparison. Current ripple has also a notable reduction in DTC-SVM compared to classic DTC. Also, at this operating point it can be seen that in classic

DTC the torque ripple of the electromagnetic torque which is resulted by the cyclic sector changes of stator flux vector and produces sharp edges, is now eliminated by using DTC-SVM.

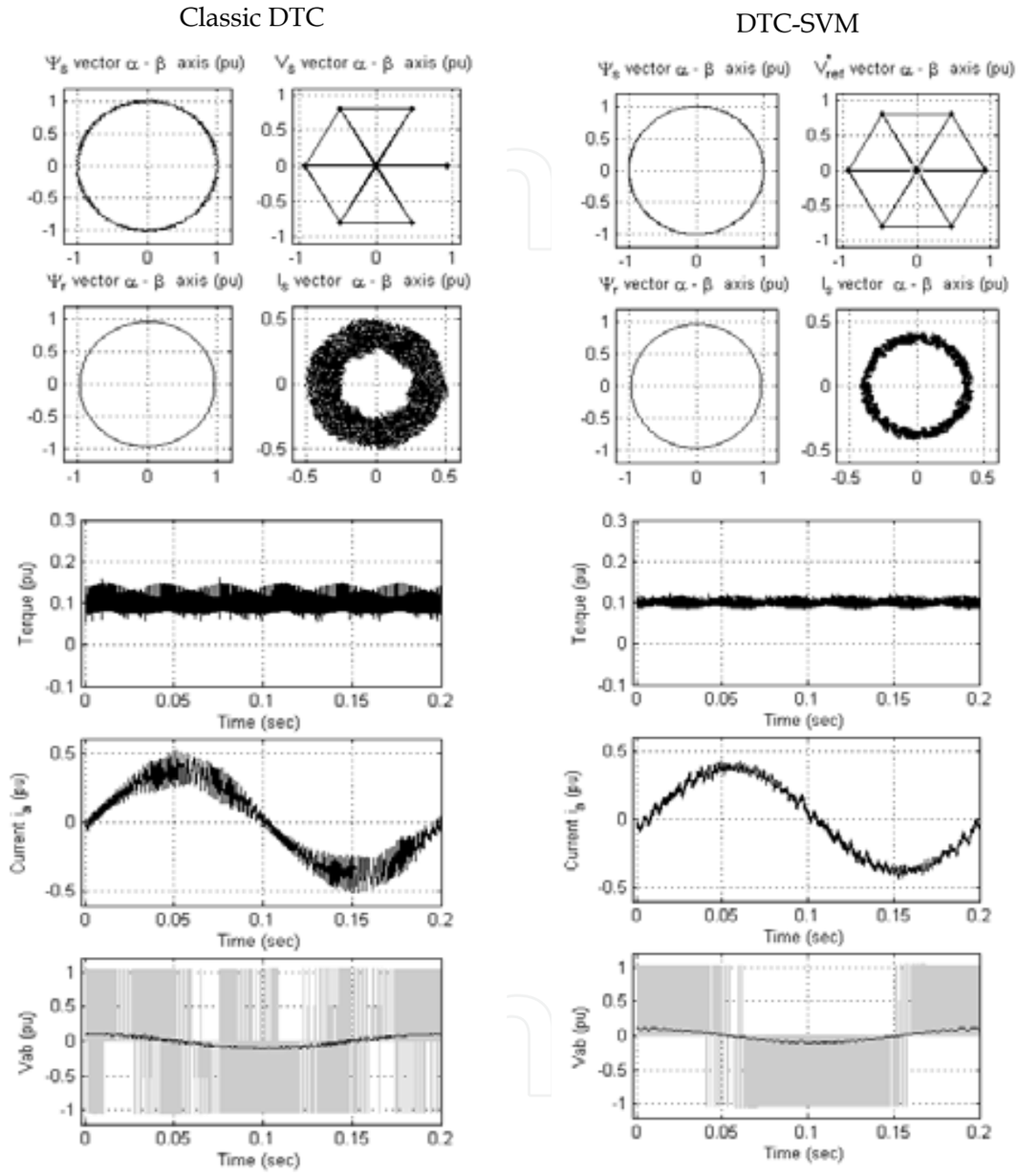

(a) (b)

Fig. 5. Steady state of the motor in an operation point where the motor has the 10% of the nominal speed and 10% of nominal load, with $HB_{\psi} = \pm 0.015$, $HB_{Te} = \pm 0.65$

(a) Classic DTC with hysteresis band controllers and $T_{S\_DTC} = 12\mu\text{sec}$ the sampling time for discrete implementation. Inverter produces 16780 states/sec.
(b) DTC with space vector modulation. Switching frequency is equal to 2.5kH and inverter produces 15000 states/sec.

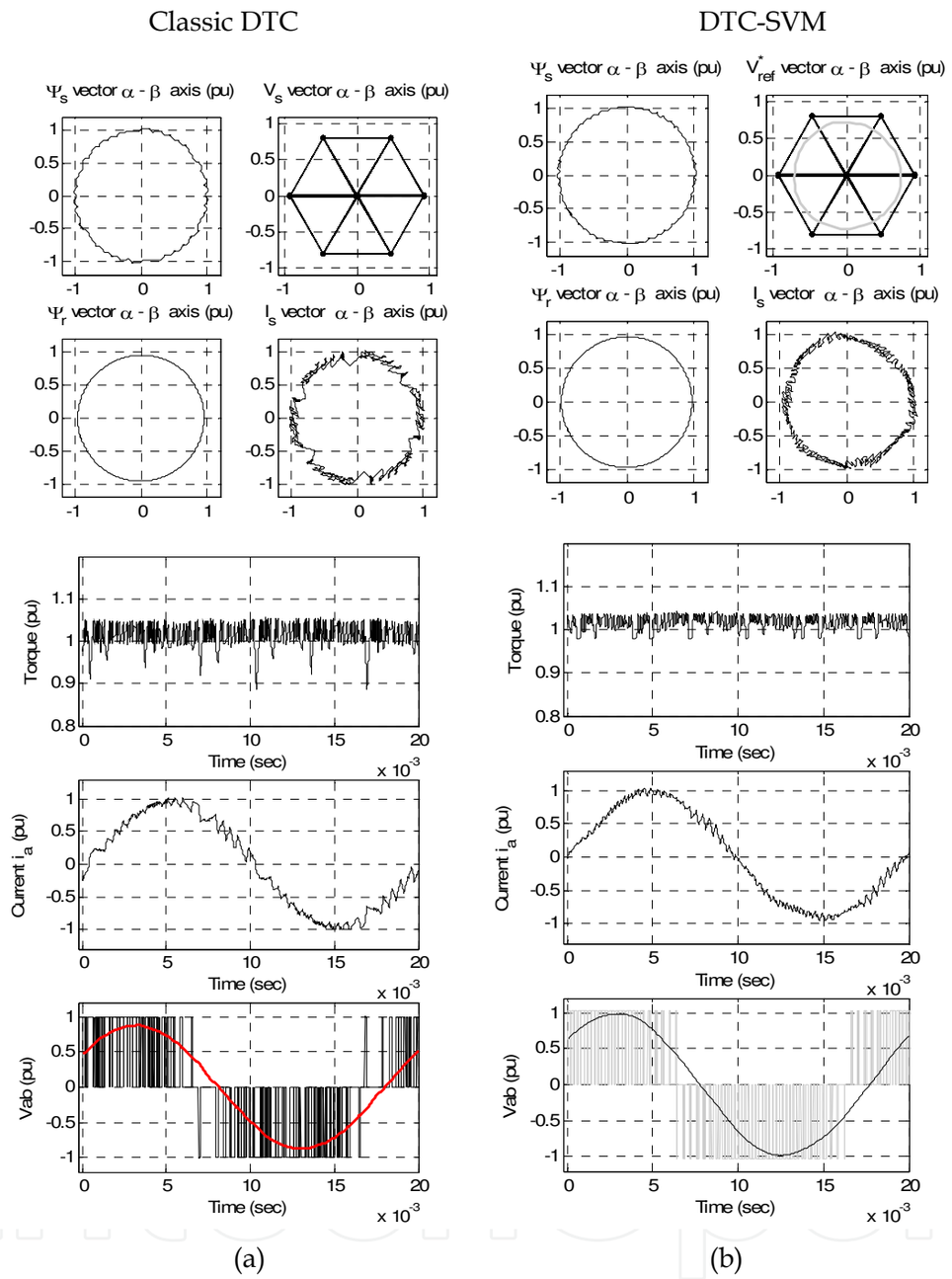

Fig. 6. Steady state of the motor in an operation point where the motor has the 100% of the nominal speed and 100% of nominal load, with $HB_{\psi} = \pm 0.015$, $HB_{Te} = \pm 0.65$ for,

(a) Classic DTC. (b) DTC with space vector modulation.

4.2 Dynamic performance of the system

In figure 7 the simulation results are presented for the dynamic case where the mechanical load is changing while the reference speed must remain constant. The case of this simulation is very rare and extreme where the motor suddenly loses the 80% of its load (from 100% to 20%) while the speed must remain constant.

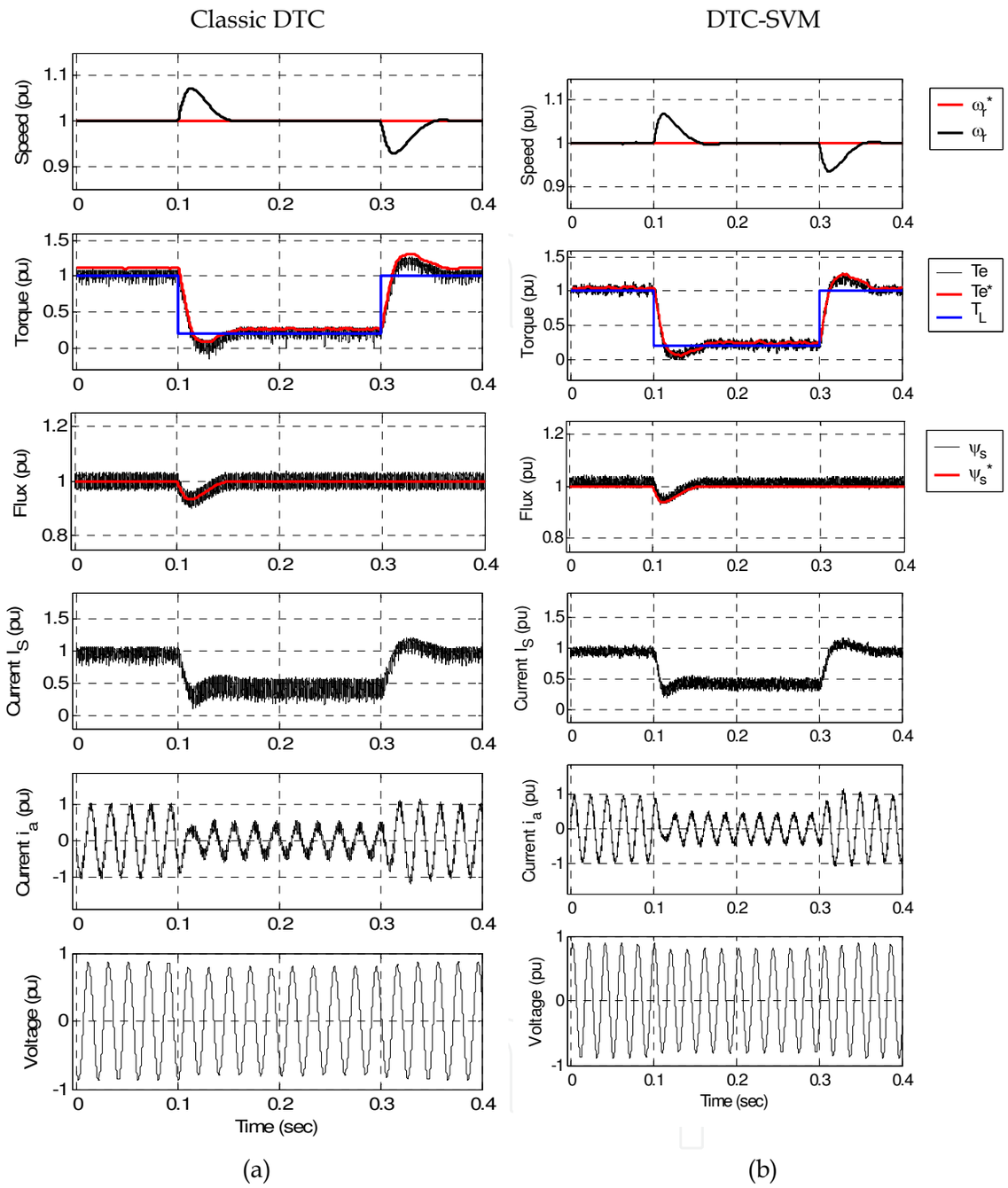

(a) (b)

Fig. 7. Load change: (a) Classic DTC, (b) DTC-SVM.

Figure 8 shows the dynamic performance of the drive system due to the reference speed step commands operation. During the transient operation of the drive system, in both cases, the ripple in electromechanical magnitudes is shown. It must be noted at this point that the speed controller, which is used for the simulations, is a fuzzy PI controller. As it is shown in figure 8 the ripple of the electromechanical magnitudes is higher in the classic DTC method in comparison to the DTC-SVM method.

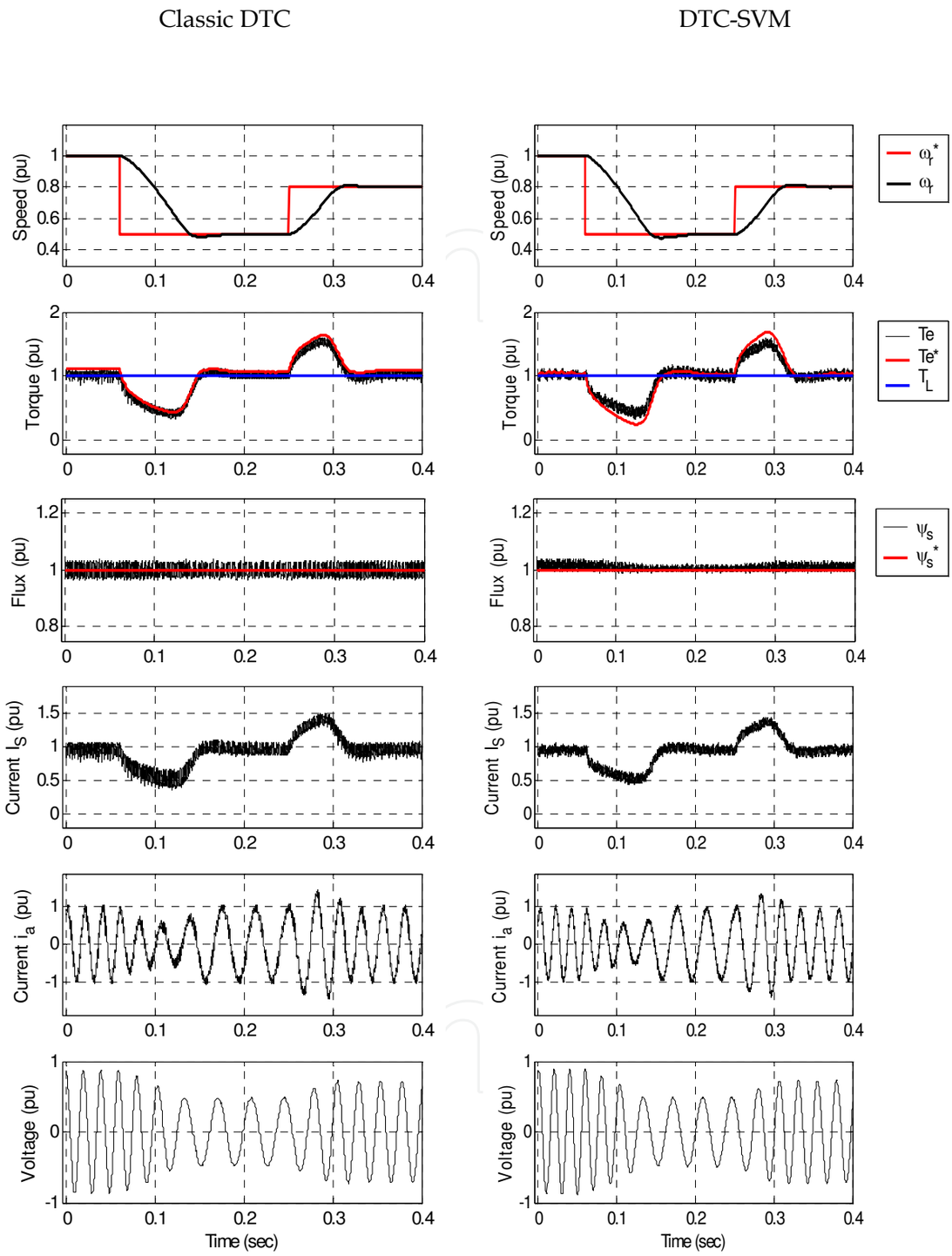

Fig. 8. Speed control response: (a) Classic DTC (b) DTC – SVM.

5. Experimental results

The implementation of the system is carried out with the development system dSPACE and the control panel R&D DS 1104 and the software package Matlab/Simulink. Also the experimental model, consists of one AC motor feed controlled converter and one DC motor feed converter which operates as a load for the system. In table II the datasheet of the experimental system kit is shown.

In figures 9a and 9b the oscillograms of the speed, torque, flux and the current components i_d and i_q of the machine are shown for reference speed variation, for both cases of control method classic DTC and DTC-SVM. In figures 10a and 10b we see the oscillograms of the electromechanical quantities of the system during load loss with classic DTC method and DTC-SVM method respectively. Where **wmegaM** is the actual value, **wref** is the reference value and the **wmega estim** is the estimated value of the angular frequency of the motor. Also the **Torque** is the actual value of the torque and the **Torque calc** is the calculated value of the electromagnetic torque. In figure 10 the **Ia ref** is the reference and **Ia** is the actual value of the DC motor's current, which is performed as a load in the experimental model. From the oscillograms it is shown that the control has more advantages in case of DTC-SVM method compared to the classic DTC.

	Asynchronous Motor	DC-Motor	Converter
Nominal Power	P_N = 2,2 kW	P_N = 4,2 kW	P_N = 4 kW
Nominal Voltage	U_N = 400 V	U_{AN} = 420 V	I_N = 7 A
Nominal Current	I_N = 4,85 A	I_{AN} = 12,5 A	
Nominal Speed	n_N = 1420 min^{-1}	n_N = 2370 min^{-1}	
Nominal power factor	$\cos\varphi_N$ = 0,82		
Number of poles	p = 4		
Stator ohmic resistance Rotor ohmic resistance	R_1 = 2,82 Ω R' = 2,78 Ω		
Stator inductance Rotor inductance of stator	L_s = 8.4 mH L'_r= 8.4 mH		
Excitation voltage		U_{EN} = 310 V	
Excitation Current		I_{EN} = 0,93 A	
Nominal Frequency			f_N = 4 kHz

Table II. Datasheets of the asynchronous motor, DC-motor and converter during the implementation

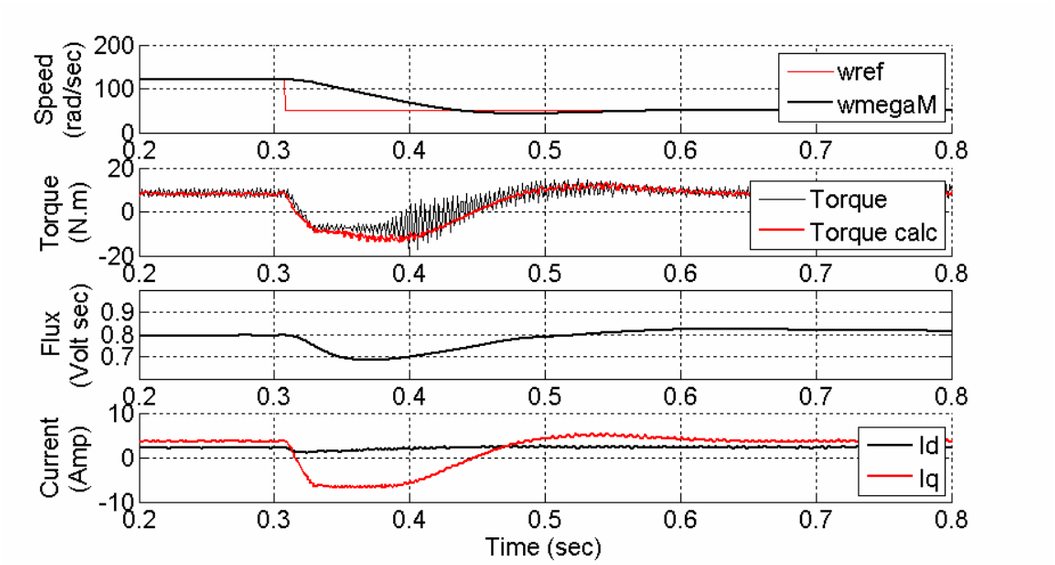

(a)

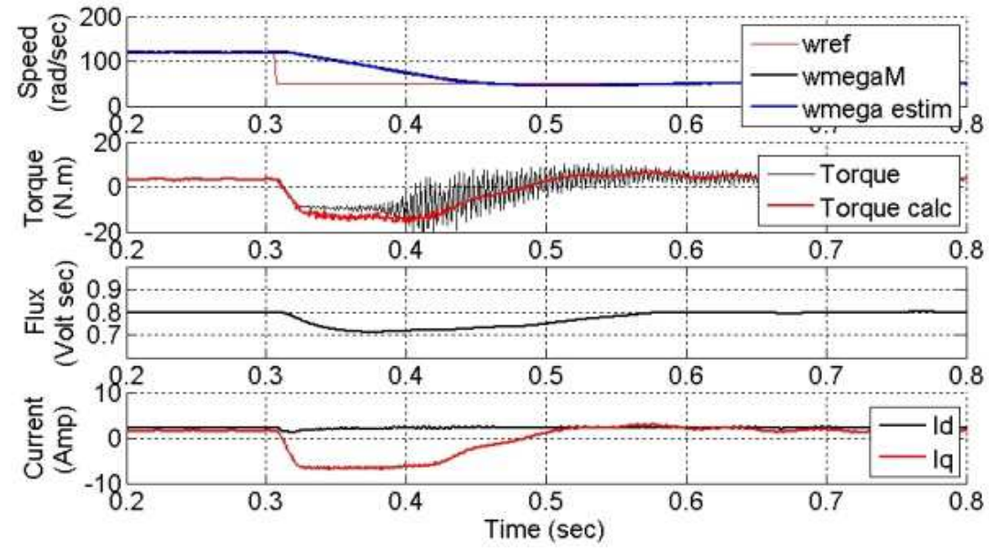

(b)

Fig. 9. Electromechanical quantities in transient operation of the system using, a) classic DTC, b) DTC-SVPWM.

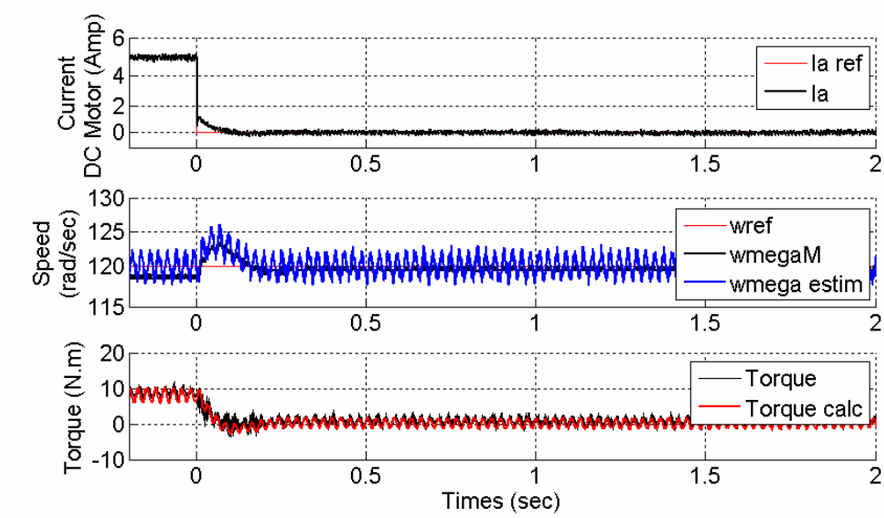

(a)

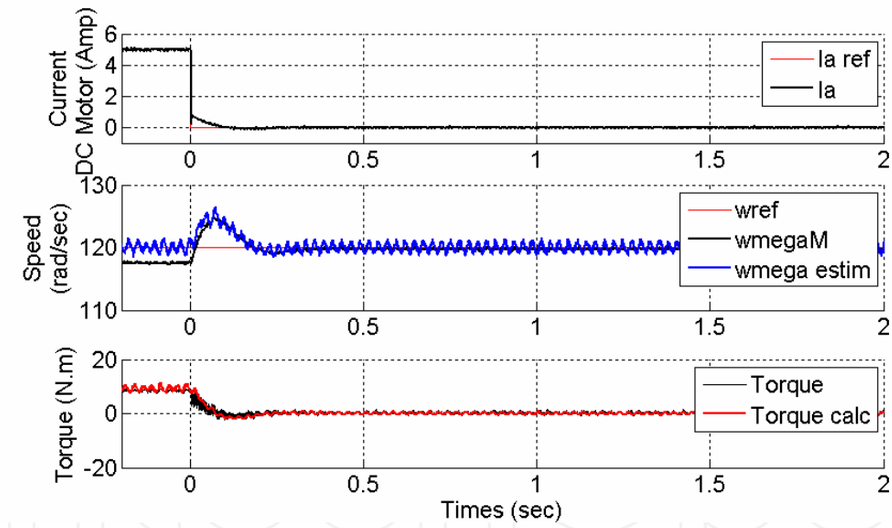

(b)

Fig. 10. Electromechanical quantities in transient operation of the system using, a) classic DTC, b) DTC-SVPWM.

6. Speed regulation using a fuzzy logic controller

So far, two methods were described for controlling the electromagnetic torque of an asynchronous motor drive. When we need to regulate the speed of such a drive a speed

controller is needed. The speed controller takes the error signal between the reference and the actual speed and produces the appropriate reference torque value. That means, the drive changes mode from torque control to speed control. So, now the mechanical load on motor shaft defines the electromagnetic torque of the motor. In torque control mode the mechanical load on motor shaft defines the rotor speed. In figure 11 we can see the block diagram of the proposed drive, in speed control mode. A reference speed signal ω_r^* or, in other words, the speed command is given. The actual speed ω_r is estimated or measured with a speed encoder. This depends on the precision requirements of each application. The speed is estimated directly from state equations. The dynamic *a-b* frame state equations of a machine can be operated to compute speed signal directly [2], [4]. Consequently, the speed computation is given by:

$$\omega_r = \frac{1}{\psi_r^2}\left[\left(\psi_{ar}\frac{d}{dt}\psi_{\beta r} - \psi_{\beta r}\frac{d}{dt}\psi_{ar}\right) - \frac{L_m}{T_r}\left(\psi_{ar}i_{\beta s} - \psi_{\beta r}i_{as}\right)\right] \tag{10}$$

Where: $T_r = L_r / R_r$

This method of speed computation requires the knowledge of the machine parameters L_r , L_m , and R_r which are the rotor inductance, the magnetizing inductance and rotor resistance respectively.

The speed controller can be a classic PI controller or a fuzzy PI controller. In [Koutsogiannis], a detailed presentation and comparison of the two controllers is presented and operates with a classic DTC drive. In this paper the fuzzy PI controller is also used for the comparison between the classic DTC and DTC-SVM.

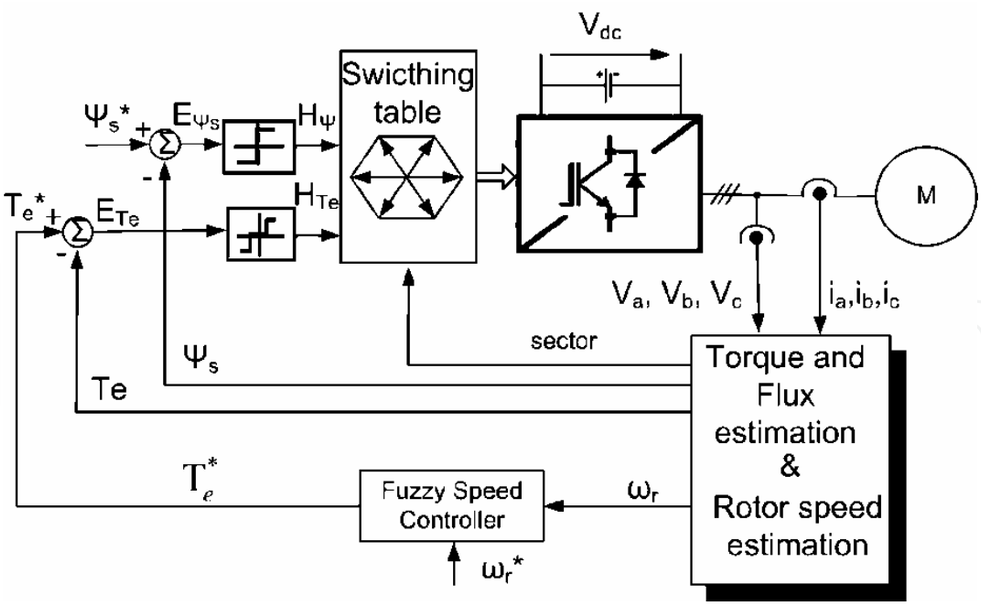

Fig. 11. Speed regulation using a speed controller.

As it will be described in the next section, the error between the estimated speed ω_r and the reference command speed ω_r^* is delivered to the speed controller, which calculates the reference electromagnetic torque T_e^* .

The corresponding output variables H_{Te}, H_{ψ} and the stator flux position sector $\theta_{\psi s}$ are used to select the appropriate voltage vector from a switching table, which generates pulses to control the power switches in the inverter. At every sampling time the voltage vector selection block chooses the inverter switching state, which reduces the instantaneous flux and torque errors.

6.1 Classic PI controller

A classic Proportional plus Integral (PI) controller is suitable enough to adjust the reference torque value T_e^*. Nevertheless, its response depends on the gains K_p and K_i, which are responsible for the sensitivity of speed error and for the speed error in steady state. During computer analysis we use a controller in a discrete system in order to simulate a digital signal processor (DSP) drive system. Its block diagram is shown in Fig.12, where T is the sampling time of the controller.

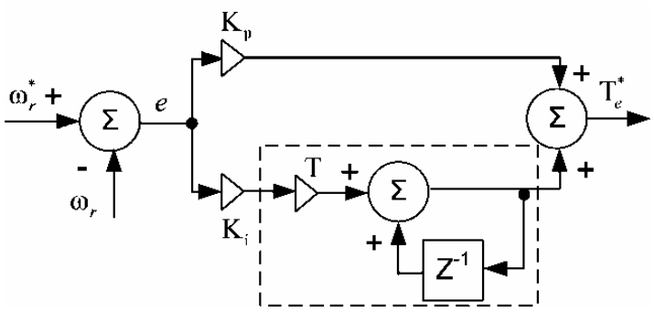

Fig. 12. Block diagram of a discrete classic PI speed controller.

The response of the PI speed controller, in a wide range area of motor speed, is very sensitive to gains *Kp* and *Ki* and it needs good tuning for optimal performance. High values of the PI gains are needed for speeding-up the motor and for rapid load disturbance rejection. This results to an undesired overshoot of motor speed. A solution is to use a variable gain PI speed controller [Giuseppe]. However, in the case of using a variable gain PI speed controller, it is also necessary to know the behaviour of the motor during start up and during load disturbance rejection in several operation points, in order to determine the appropriate time functions for PI gains. This method is also time-consuming and depends on the control system philosophy every time. To overcome this problem, we propose the use of a fuzzy logic PI controller.

6.2 Fuzzy PI controller

Fuzzy control is basically an adaptive and nonlinear control, which gives robust performance for a linear or nonlinear plant with parameter variation. The fuzzy PI speed controller has almost the same operation principles with the classic PI controller. The basic difference of the two controllers is that the output of the fuzzy PI controller gives the change in the reference torque value dT_e^*, which has to be summed or intergraded, to give the T_e^* value (Fig.13). The FL controller has two inputs, the speed error $E = \omega_r^* - \omega_r$ and the change in the speed error CE, which is related to the derivative dE/dt of error. In a discrete system, assuming $dt = T$, where T is the constant sampling time of the controller, $CE = \Delta E$. Fuzzy controller computes, for a specific input condition of the variables, the output signal.

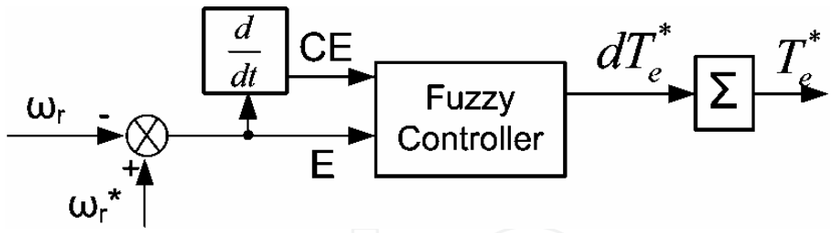

Fig. 13. Basic block diagram of a fuzzy PI speed controller.

All in all, the fuzzy controller is an input/output static nonlinear system which maps the pair values of *E* and *CE* according to fuzzy rules (Table III) and gives the following form:

$$K_1 E + K_2 CE = dT_e^* \tag{11}$$

Where, K_1 and K_2 are nonlinear gain factors.

The analytical block diagram of the fuzzy PI controller is shown in Fig. 14. The input variables *E* and *CE* are expressed in per unit values. This is achieved by dividing the variables by specific scale factors. The output will also be expressed in per unit values. The advantage of fuzzy control in terms of per unit variables is that the same control algorithm can be applied to all the plants of the same family. Generally, the scale factors can be constant or programmable. Programmable scale factors control the sensitivity of operation in different regions of control.

The fuzzy rules of the controller are based in linguistic expressions from the physical operation of the system. As mentioned before, the output of the controller is the change in the reference torque value dT_e^* . The fuzzy sets of linguistic expressions of the variables and the membership functions (MFs) of these variables are shown in Fig.15 (a),(b). As mentioned before, the output of the controller is the change in the reference torque value dT_e^*. The MFs of the output variable in per unit values are shown in Fig.15(c). The definition of the MFs depends on the system behavior. All the MFs are asymmetrical because near the origin (steady state), the signals require more precision.

The next step in the analysis of fuzzy speed controller is the definition of fuzzy rules. The fuzzy rules for the speed controller are shown in Table III. We can see that the top row and the left column of the matrix indicate the fuzzy sets of the variables e and ce , respectively, and the MFs of the output variable $dT_e^*(pu)$ are shown in the body of the matrix. There may be 7 x 7 = 49 possible rules in the matrix, where a typical rule reads as:

$$IF \;\; e(pu) = PS \;, \quad AND \; ce(pu) = NM \;, \quad THEN \;\; \Delta T_e^*(pu) = NVS \tag{12}$$

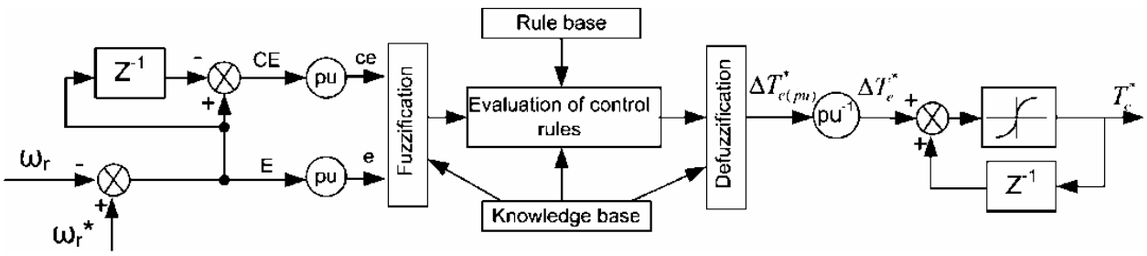

Fig. 14. An analytical discrete block diagram of the fuzzy PI controller.

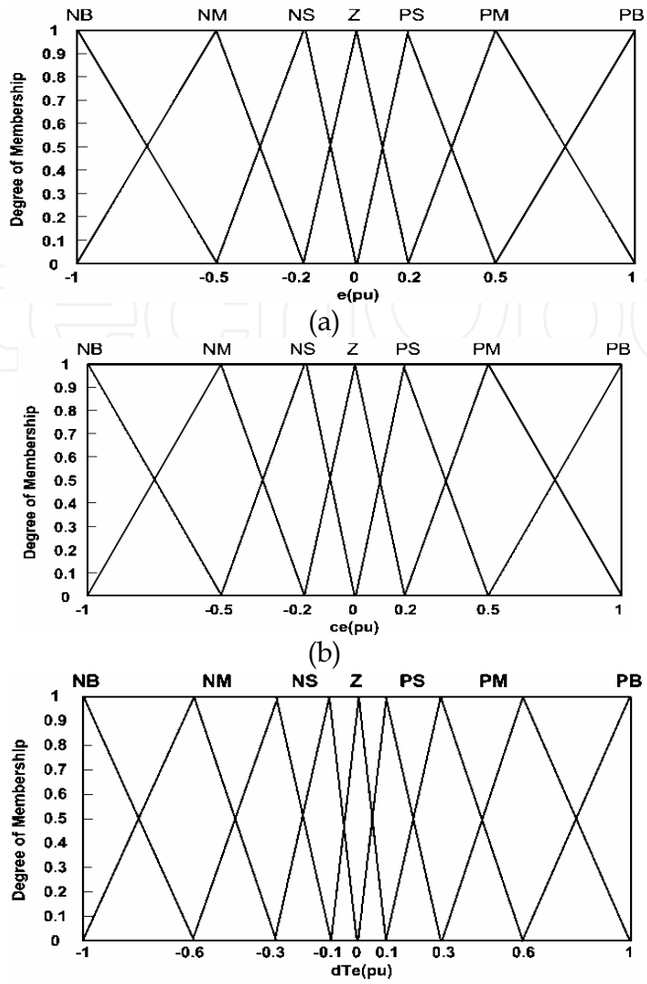

Fig. 15. Membership functions of the input variables (a) speed error e(pu) (b) change in speed error ce(pu) and of the output variable (c) change in reference torque value ΔTe* of the fuzzy PI speed controller.

e(pu) / ce (pu)	NB	NM	NS	Z	PS	PM	PB
NB	NB	NB	NB	NM	NS	NVS	Z
NM	NB	NB	NM	NS	NVS	Z	PVS
NS	NB	NM	NS	NVS	Z	PVS	PS
Z	NM	NS	NVS	Z	PVS	PS	PM
PS	NS	NVS	Z	PVS	PS	PM	PB
PM	NVS	Z	PVS	PS	PM	PB	PB
PB	Z	PVS	PS		PB	PB	PB

where, PB = Positive Big, PM = Positive Medium, PS = Positive Small, PVS = Positive Very Small, Z = Zero, NVS = Negative Very Small, NS = Negative Small, NM = Negative Medium, NB = Negative Big.

Table III. Fuzzy Rules

The implication method that we used in simulations is the Mamdani type. There are many types of fuzzy logic controllers, but now the classical structure of Mamdani type is used.

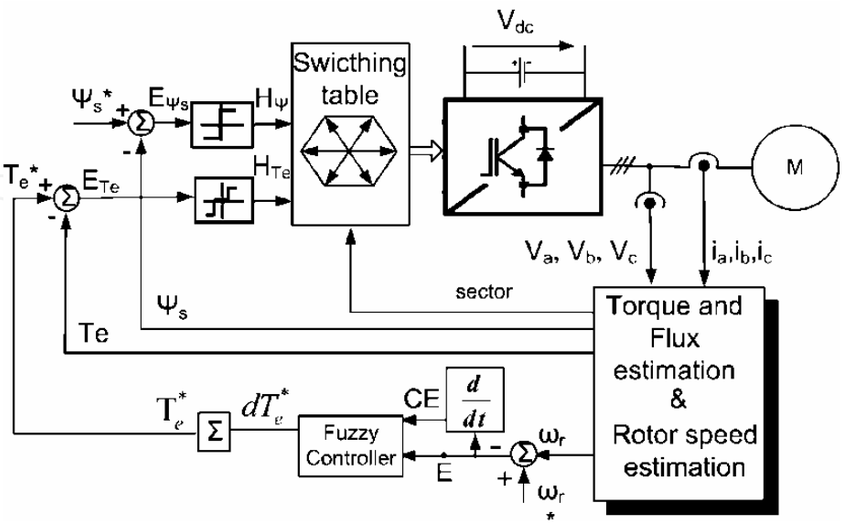

Fig. 16. DTC block diagram with fuzzy logic controller.

The rule matrix and MF description of the variables are based on the knowledge of the system. Summing up, the setting of the fuzzy controller depends on the system requirements for optimal performance. When the fuzzy speed controller is well tuned its performance is excellent in a wide range of motor speed. Fig 16 shows the block diagram of Direct Torque Control Induction Motor Drive using a Fuzzy Speed Controller.

6.3 Simulation results

In this paragraph, the simulation results of a system using the classic PI speed controller (Fig.17.I) and the fuzzy PI speed controller (Fig.17.II) are presented. For the needs of simulation, we used an 160kW, 400V, 50Hz, 1487rpm, $R_s = 0.01379\Omega$ induction motor which is fed by a VS inverter using the DTC method. In more detail the parameters of motor are shown in Table IV,

P=4(2 pair of poles), f=50 Hz	R_s=0,0137 Ω	L_s=0,007705 H
230V/400V	$R_r = 0.00728\Omega$	L_s=0,007705 H
P=160kW, $N_r = 1487$ rpm	L_m=0,00769 H	
J=0.02 Kgm^2	F=0,05658 Nms	

Where J is the machine's inertia, and F is the friction factor.

Table IV. Induction Machine Parameters

To simulate the drive we used Matllab/Simulink software. The DTC sampling time was 30μs and the speed controller sampling time was 3ms. The reference stator flux magnitude was constant at 1.02 Wb. Fig.17(I) shows the dynamic performance of the DTC-SVM drive using a classic PI speed controller. The results of Fig.17 show that the startup of the motor, until it reaches the command speed value 600 rpm, is made with 400 Nm initial load torque. When the motor runs at 600 rpm/400Nm steady state operation, a step speed command of

1200 rpm is given to the drive and the motor reaches again another operation point (1200rpm/400Nm). Finally, the controllers are tested to step load torque disturbance. It is easy, therefore, to come to the conclusion that fuzzy speed controller has a remarkably better response than the classic PI speed controller.
The system was also investigated during the starting period and its control under different commutative periods. In this fig. 17 it is shown that the torque of the motor has lower ripple when the speed estimation is being carried out using a fuzzy PI controller.

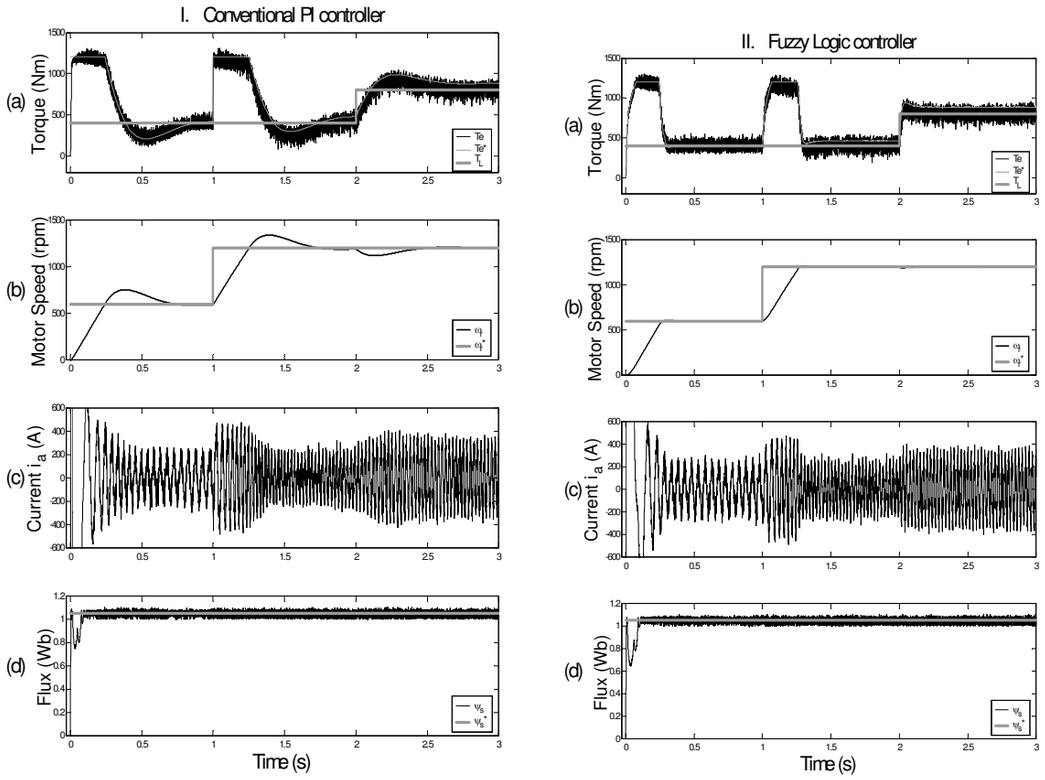

(a) (b)

Fig. 17. Motor control response with steps of speed command and load torque. (a) Electromagnetic torque T_e, speed controller output T_e^*, load torque *TL,* (b) actual motor speed ω_r, reference speed ω_r^*,(c) stator current i_{sa} in phase a (d) stator flux magnitude Ψ_s, *and* reference value Ψ_s^*.

Fig. 18 shows, in more detail, the comparison of the motor speed response using the two different speed controllers, during steps of speed command ω_r^* and load torque. To investigate the system for the classic PI controller more than one pairs of values Kp and Ki have been used. The two controllers were tested in a wide range of engine speed. Extending, namely, from a very low speed to a very high speed of the motor. It was observed, that the fuzzy PI controller has better performance than the classic PI controller.
In fig. 19 we observe that the acceleration of the motor using the classic PI speed controller is almost the same, independently of command step, and generally a linearity is observed, which depends only on the load on the axis of motor. In other words we have the maximum acceleration of the motor under these conditions. This means that when we have a small

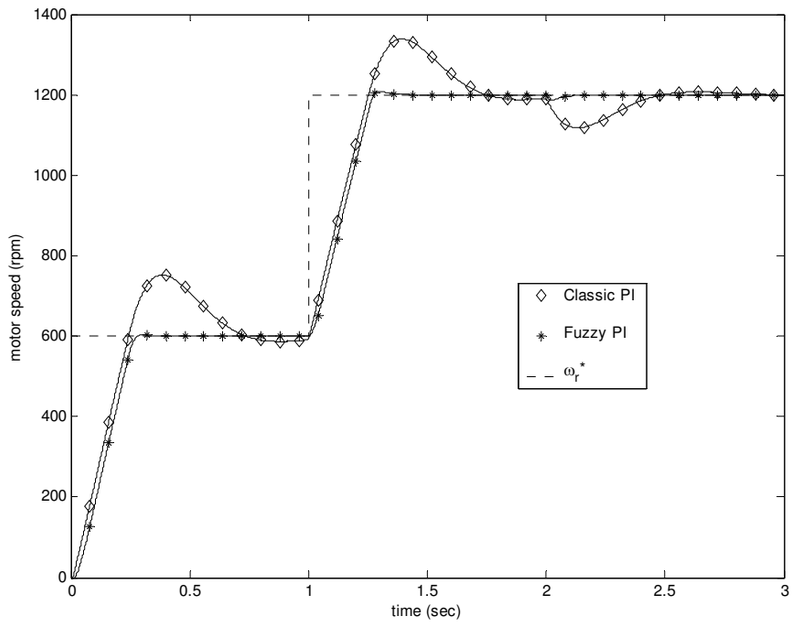

Fig. 18. Motor speed control response with steps of speed command and load torque.

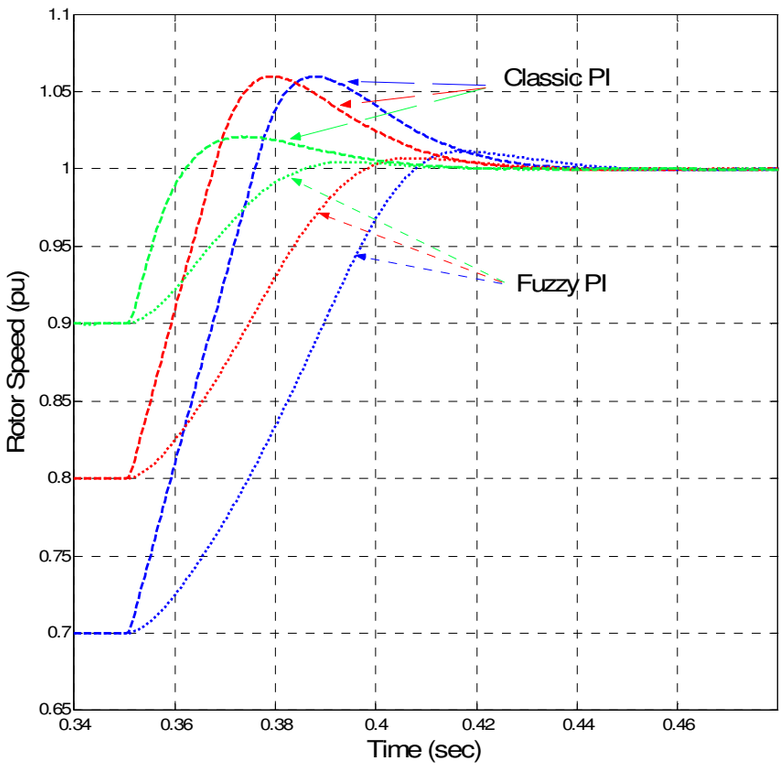

Fig. 19. Dynamic behaviour of classic PI and Fuzzy PI controller during motor startup. Load in the shaft of the motor equal with 50% nominal and various step changes of speed.

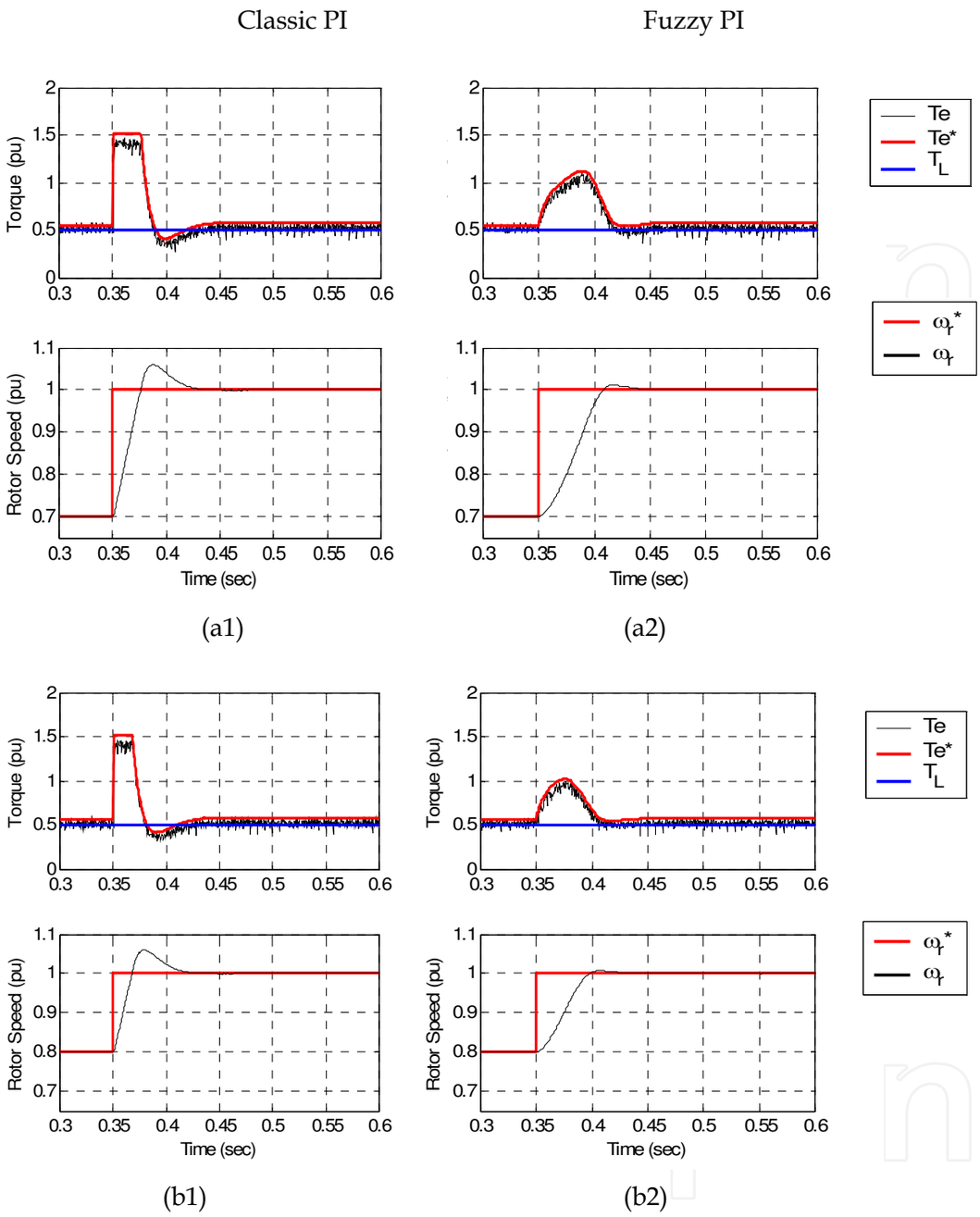

Fig. 20. Simulation results of the speed controller response in various speed step commands. (1) Classic PI controller, (2) Fuzzy PI controller. (a) 30%, (b) 20%

load in the shaft of the motor and the step is small, then an overshoot in the speed of the motor is observed. On the contrary, with the fuzzy PI of controller, we observe an acceleration that depends on the step of command and the load on the shaft. In fig. 20 an analytical comparison of the dynamic performance of the control system is presented. The system behavior can be studied when the motor speed increases, while the load torque in the motor shaft remains constant at 50% of the nominal load. In more detail, the dynamic

performance of the two speed controllers, classic PI and fuzzy PI, is presented during increase of the motor speed by 30%, 20% and 10% step commands of the nominal speed respectively. In this figure, the improvement in motor acceleration and the change in motor torque using the fuzzy PI controller can be seen. Classic PI controller shows an undesirable overshoot of the actual speed. On the other hand, fuzzy PI controller has a smoother response. The output of each controller is the value of the reference electromagnetic torque T_e^* . The change in motor speed is the result of applying the produced reference torque to the DTC scheme.

7. Direct torque control for three level inverters

7.1 Control strategy of DTC three-level inverter

The applications of inverter three or multiple level inverters have the advantage of reducing the voltage at the ends of semiconductor that mean the inverters can supply engines with higher voltage at the terminals of the stator. Also, the three level inverters show a bigger number of switching states. A three level inverter shows 3^3=27 switching states. This means an improvement in the higher harmonics in the output voltage of the inverter and hence fewer casualties on the side of the load and less variation of electromagnetic torque. In direct torque control for a two-level inverter there is no difference between large and small errors of torque and flux. The switching states selected by the dynamics of drive system with the corresponding change of desired torque and flux reference is the same as those chosen during the operation in steady state. For the three-level voltage inverter is a quantification of the input variables. In this case, increasing the torque on the control points of the hysteresis comparators in five (Figure 21) and the three magnetic flux (Figure 22). Also divided the cycle recorded by electromagnetic flow of the stator in a rotating, in 12 areas of 30^o as shown in Figure 23. This combined with the increased number of operational situations, for three-level inverter is 27 and is expressed in 19 different voltage vectors can be achieved better results. Figure 24a shows the 19 voltage vectors for the three level voltage source inverter of figure 25, and the vector of magnetic flux of the stator Ψs. It should be noted that in Figure 24a vectors V1, V2, V3, V4, V5, V6 shown each for two different operating conditions and the zero vector V0 for three different situations. The angle the vector i in relation to the axis a is less than 30^o. The possible changes in magnetic flux stator which can be achieved using the voltage vectors of operating conditions shown in 24b.

From Figures 24.a and 24b seems to change the value of stator flux **Ψs** in a new value should be selected the following voltage vectors. If an increase in the flow can be achieved by applying one of the voltage vectors **V9, V2, V8, V1, V7,** because in this case, the new vector of stator flux will be correspondingly **Ψs+ΔΨ9, Ψs+ΔΨ2, Ψs+ΔΨ8, Ψs+ΔΨ1, Ψs+ΔΨ7.** By the same token if we can achieve a reduction of magnetic flux should implement one of the voltage vectors **V14, V5, V15,** since in this case the new vector of stator flux is **Ψs+ΔΨ14, Ψs+Ψ5, Ψs+ΔΨ15,** which is less than the original **Ψs.** Also for the electromagnetic torque, taking into account the equation 6, if is necessary very sharp increase in torque, then we can apply one from the voltage vectors **V11, V3, V12** because it will grow along with the flow and the angle between the vectors δ of stator flux and the rotor. If a reduction of the torque is needed we can apply one from the voltage vectors **V6, V17, V18.** By the same token if is required large increase in flow and a slight increase in torque can do a combination of the above and apply the vector **V8** or if stator magnetic flux is constant and requires a small reduction of the torque is needed can be chosen one from

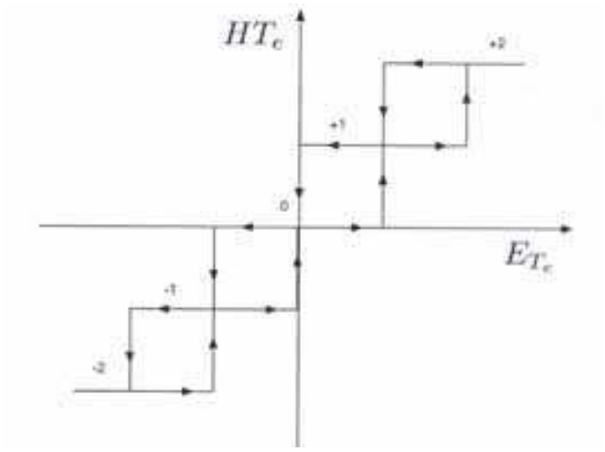

Fig. 21. Hysteresis comparator 5 level for the electromagnetic flux

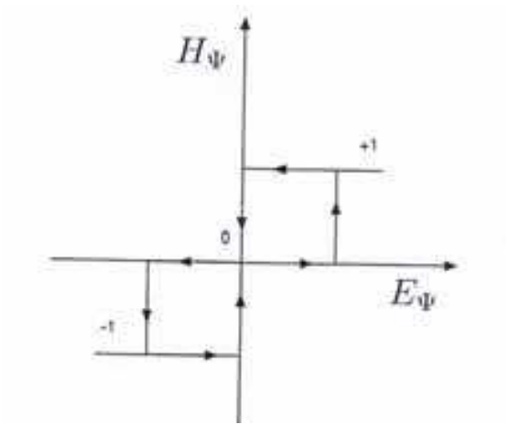

Fig. 22. Hysteresis comparator 3 level for the magnetic flux

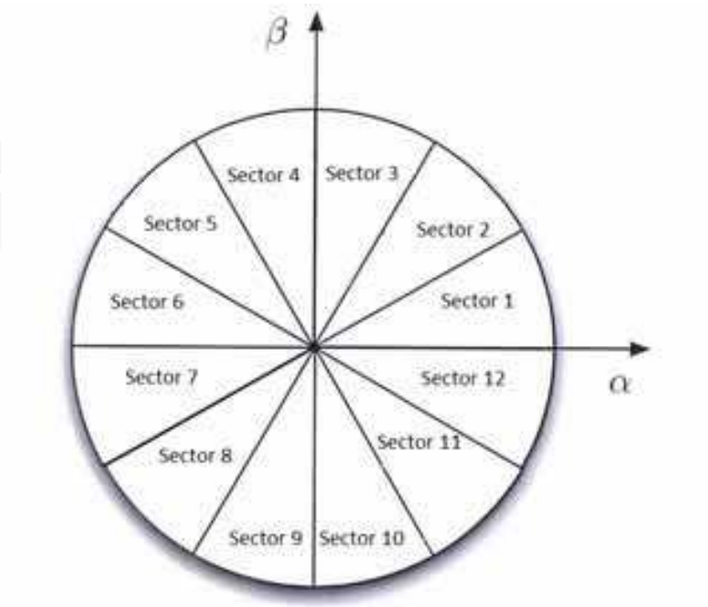

Fig. 23. Sectors of Statorsmagnetic flux.

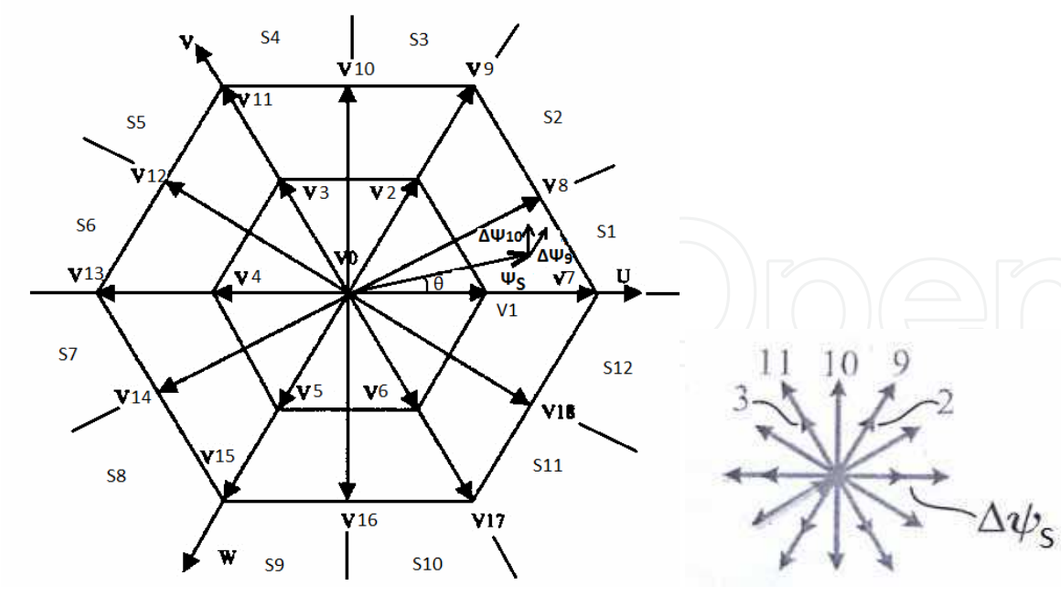

(a) (b)

Fig. 24. a) voltage vectors of 3 level voltage b) changes of the stator's flux with the vector of each switching state.

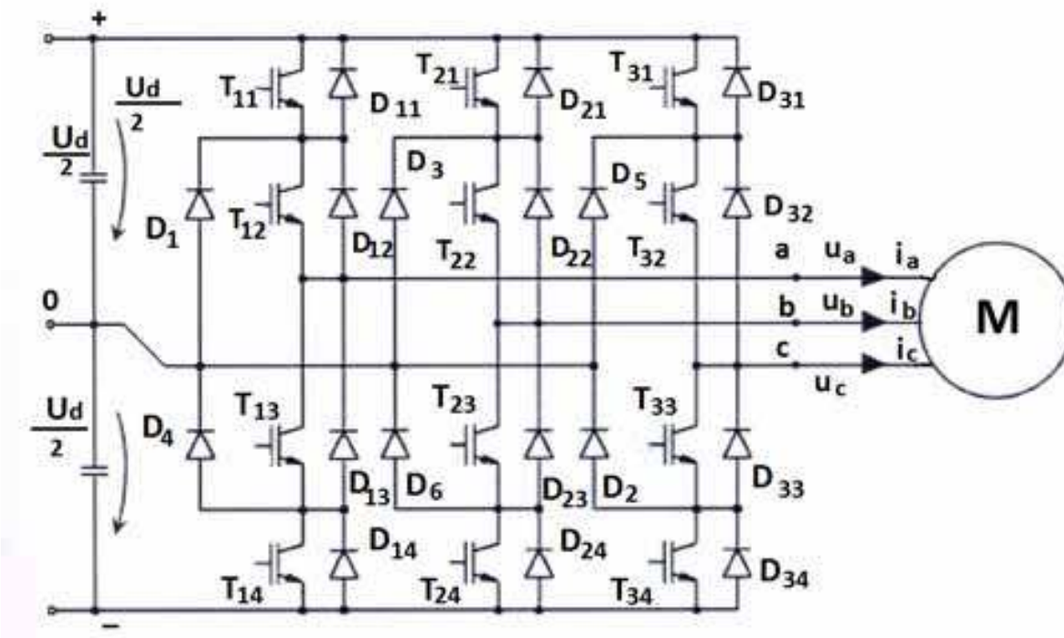

Fig. 25. Three- level voltage source inverter

zero voltage vectors **V0**. Of course the number of vectors that can bring the desired change in magnetic flux in stator and electromagnetic torque varies to the angle the vector of magnetic flux on the axis A. As is natural in such cases there are other suitable candidate voltage vectors. The correct choice of the vectors, depending on the desired change in the flow and torque that we want to do, depending on the sector in which the vector of the flow,

it is the biggest challenge to build such a table in direct torque control for drive systems powered by three-level voltage inverters. So the inverter three-level table is not widely accepted for pulsing as in the case of two-level inverters.
Based on the above logic while taking into account the intersection of Figure 3 in which may be in the vector of the stator magnetic flux, it became the table I.

Flux(ψ_S)	Torque(T_e)	S1	S2	S3	S4	S5	S6	S7	S8	S9	S10	S11	S12
	-2	V0	V0	V0	V0	V0	V0	V0	V0	V0	V0	V0	V0
	-1	V3	V4	V4	V5	V5	V6	V6	V1	V1	V2	V2	V3
-1	0	V3	V4	V4	V5	V5	V6	V6	V1	V1	V2	V2	V3
	1	V11	V12	V13	V14	V15	V16	V17	V18	V7	V8	V9	V10
	2	V11	V12	V13	V14	V15	V16	V17	V18	V7	V8	V9	V10
	-2	V0	V0	V0	V0	V0	V0	V0	V0	V0	V0	V0	V0
	-1	V2	V3	V3	V4	V4	V5	V5	V6	V6	V1	V1	V2
0	0	V2	V3	V3	V4	V4	V5	V5	V6	V6	V1	V1	V2
	1	V10	V11	V12	V13	V14	V15	V16	V17	V18	V7	V8	V9
	2	V10	V11	V12	V13	V14	V15	V16	V17	V18	V7	V8	V9
	-2	V0	V0	V0	V0	V0	V0	V0	V0	V0	V0	V0	V0
	-1	V2	V3	V3	V4	V4	V5	V5	V6	V6	V1	V1	V2
1	0	V2	V3	V3	V4	V4	V5	V5	V6	V6	V1	V1	V2
	1	V9	V11	V11	V13	V13	V15	V15	V17	V17	V7	V7	V9
	2	V9	V11	V11	V13	V13	V15	V15	V17	V17	V7	V7	V9

Table I

7.2 Simulation of the system in the computer

The drive system considered consists of three-phase asynchronous motor, three phase three level voltage inverter and control circuit with hysteresis comparators electromagnetic torque and flux of Figures 21 and 22 respectively. The system design was done by computer simulation with Matlab / Simuling. Figure 26 shows the general block diagram of the simulation.
By simulating the drive system on the computer can pick up traces of electromechanical sizes in both permanent and transition state in the system. From the curves can be drawn for the behavior of both the load response and the response speed. Details of the induction motor and inverter with three levels that will make computer simulations are shown in Tables II and III respectively.

7.3 Simulation resuls

In this text we will present the waveforms of electromechanical changes in the size of the load. To investigate the behavior of the electric drive system in response to load change incrementally load of 25 Nm to 30Nm, then by 30Nm to 25 Nm, maintaining the engine speed steady at 1000 rpm. Figure 27 shown the electromagnetic torque and Figure 8, the engine speed according to the time when the transition state in which they affect the load.

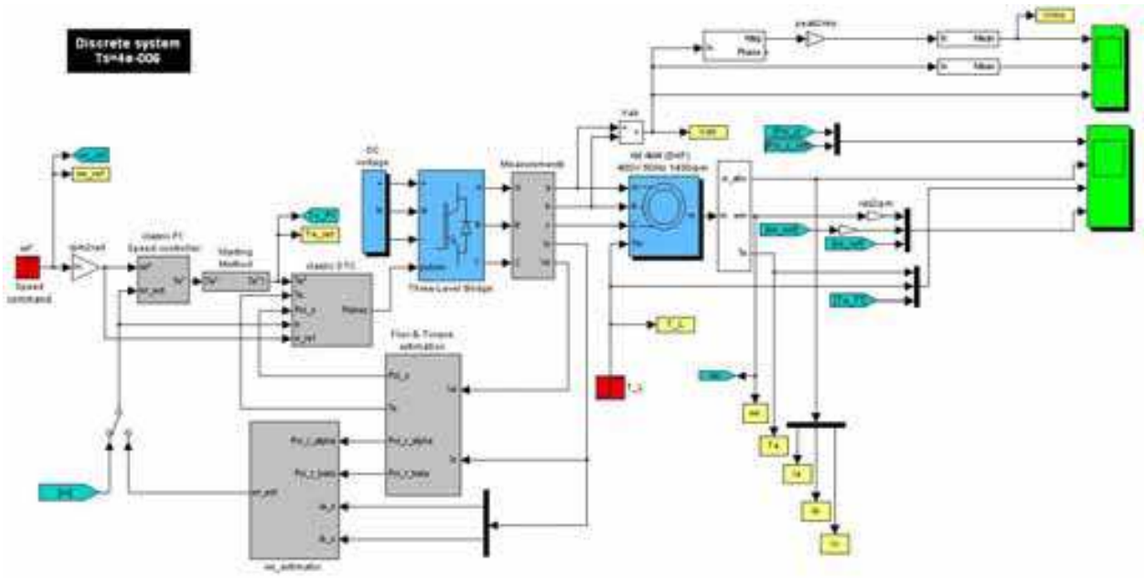

Fig. 26. Block diagram DTC Three-level Inverter in the Simulink with speed estimator.

Nominal power	**P = 4000W**
Stator phase voltage	**V = 460 V**
Ohmic resistance of stator	**R_s = 1.405 Ω**
Ohmic resistance of rotor	**R_r = 1.395 Ω**
Main magnetic induction	**L_m = 172.2x10^{-3} H**
Stator leakage inductance	**L_{ls} = 5.84x10^{-3} H**
Motor leakage inductance	**L_{lr} = 5.84x10^{-3} H**
Leakage torque	**J = 0.0131 Kg.m^2**
Coefficient of friction	**F = 0.002985 Nms**
Number of poles	**P = 4 (two pairs of poles)**

Table II. Nominal details of induction motor

Semiconductor	**IGBT with antiparallel diodes**
Ohmic resistance Snubber	**R_s = 1000 Ω**
Capacitance Snubber	**C_s = infinite**
Internal resistance semiconductor	**Ron = 0.001 Ω**
IGBT voltage crossing	**V_f = 0.8 V**
Diode voltage crossing	**V_f = 0.8 V**

Table III. Nominal details of inverter

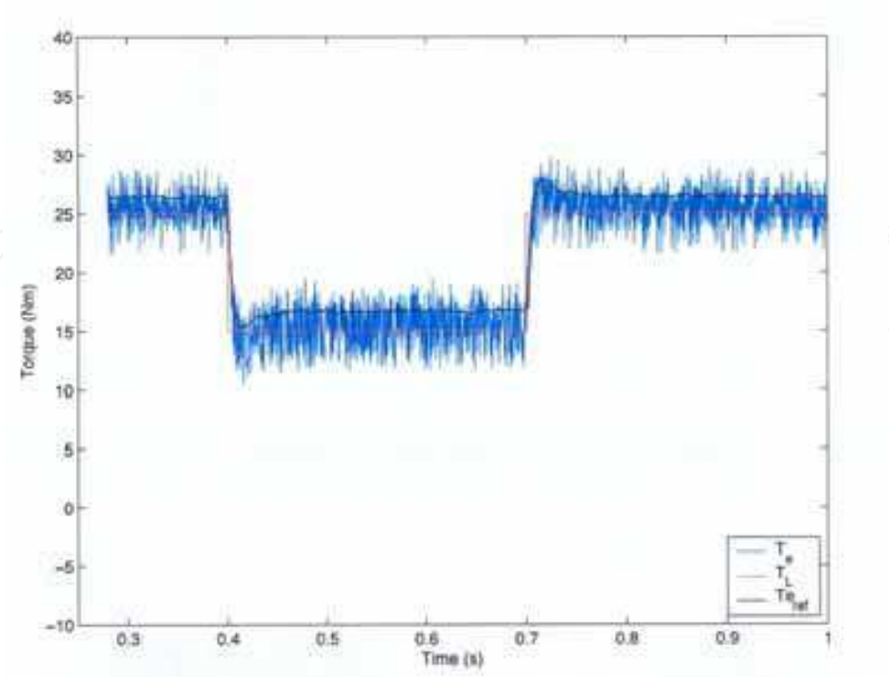

Fig. 27. Electromagnetic flux, reference flux and load flux versus time

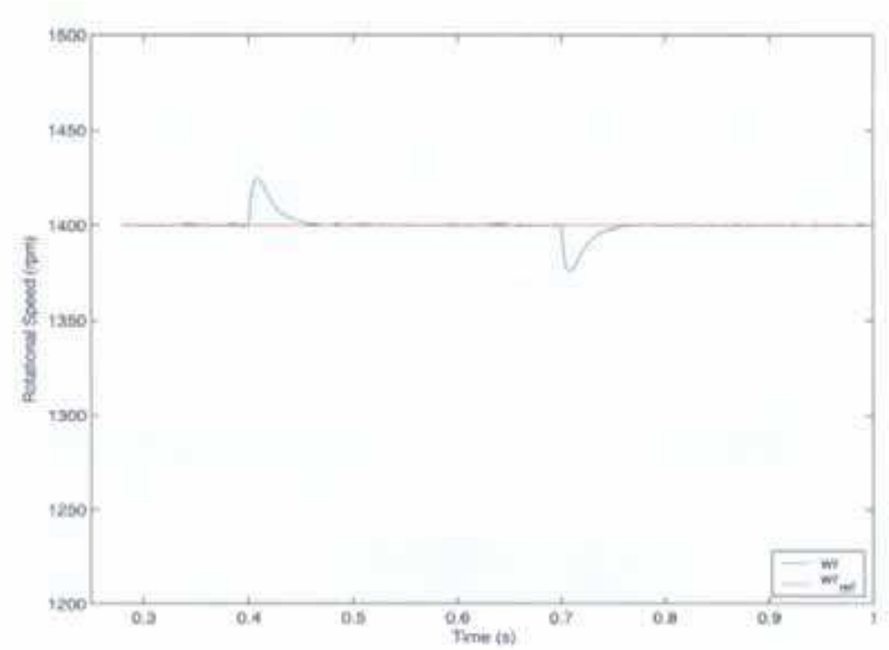

Fig. 28. Speed reference and actual speed versus time

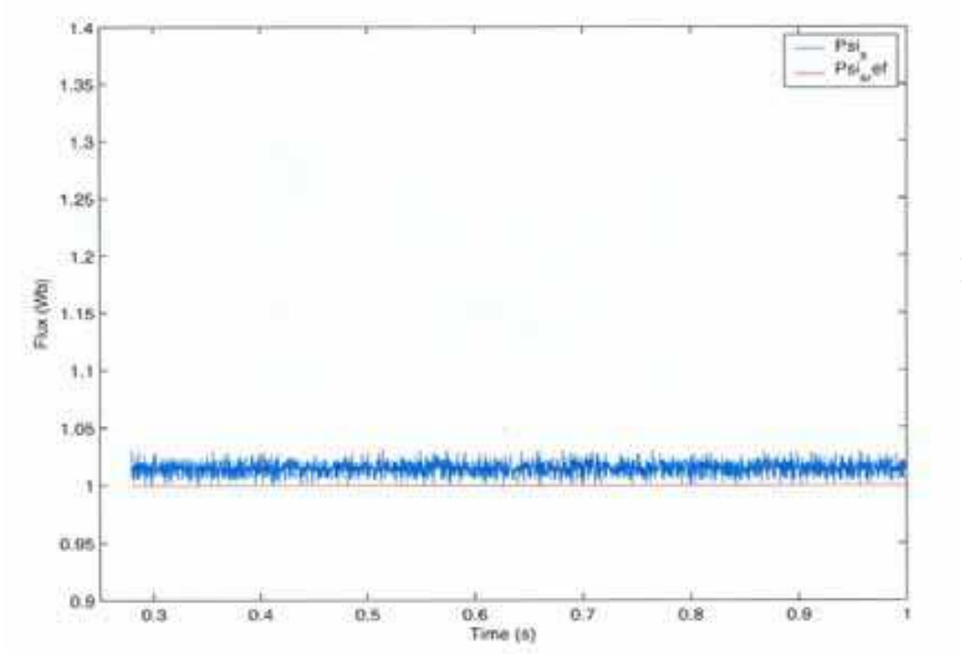

Fig. 29. Electromagnetic stator flow versus time.

By changing the load observed a slight, temporary change of speed. Figure 9 shows the change of the stator flux versus time and Figure 30 is the change of magnetic flux in the stator three-axis system that is α,β system versus time. Figure 31 shows the change of the vector current in the stator system. In this figure shows the change of the modulus of vector power to change the load. When the torque load is reduced and the measure of the vector current and increase the vector of power when the load increases.

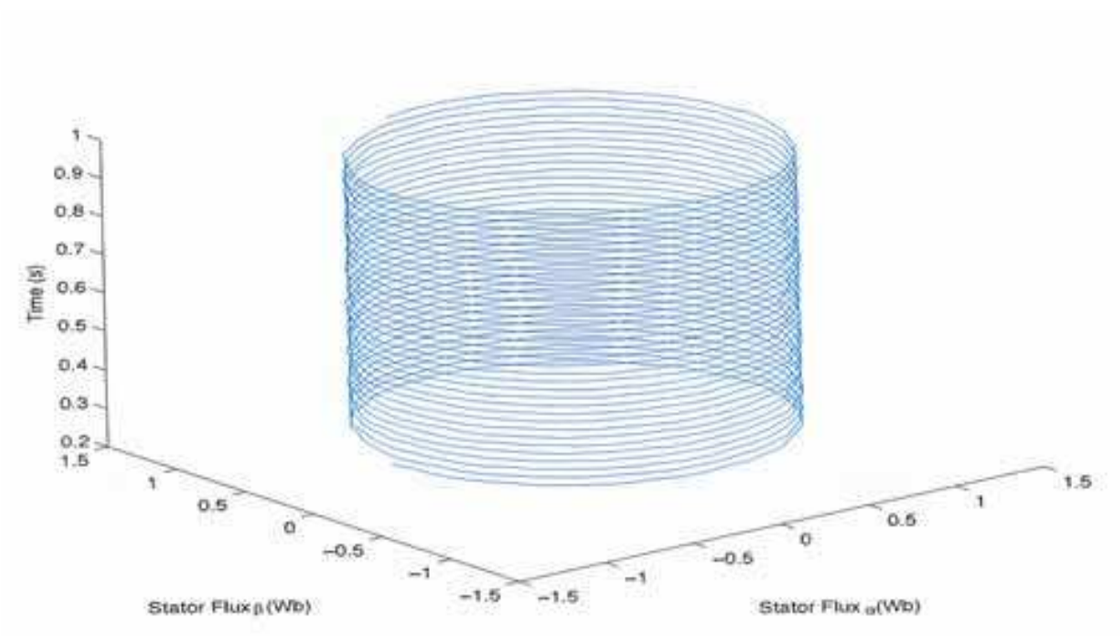

Fig. 30. Electromagnetic flow in the stator ιν α,β system is a function of time

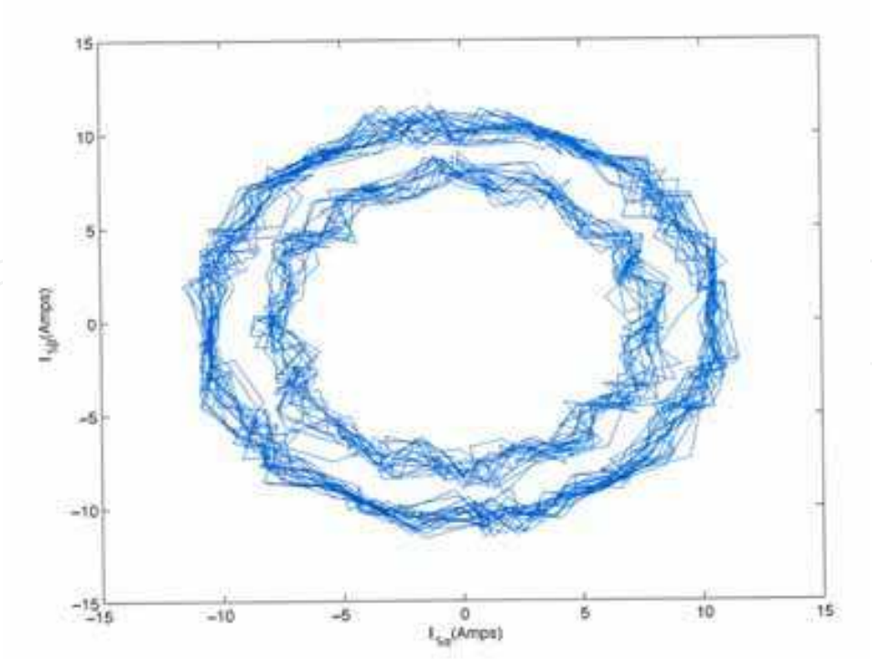

Fig. 31. Current in the stator in α,β reference system

8. Conclusion

This paper has presented a modified Direct Torque Control method for PWM-Inverter fed asynchronous motor drive using constant switching frequency. Constant-switching-frequency is achieved by using space vector modulation and finally, an SVM based DTC system, compared to the classic DTC scheme for torque control. DTC-SVM schemes improve considerably the drive performance in terms of reducing torque and flux pulsations, reliable startup and low-speed operation, well-defined harmonic spectrum, and radiated noise. Therefore, DTC-SVM is an excellent solution for general-purpose asynchronous motor drives. On the contrary, the short sampling time required by the classic DTC schemes makes them suited to very fast torque- and flux-controlled drives because of the simplicity of the control algorithm. When a speed control mode instead of torque control is needed, a speed controller is necessary for producing the reference electromagnetic torque value. For this purpose a fuzzy logic based speed controller is used. Fuzzy PI speed controller has a more robust response, compared to the classic PI controller, in a wide range area of motor speed.

9. References

Takahashi I. & Noguchi T.(1986): *A new quick-response and high efficiency control strategy of an induction machine*, IEEE Trans. Ind. Applicat., vol. 22, pp. 820–827, Sep./Oct.

Bimal K. & .Bose (2002). *Modern Power Electronics And AC Drives*. Prentice Hall.

Andrzej M. & Trzynadlowsky (2002).*Control of Induction Motors*. Academic Press.

Boldea I. &.Nasar S.A. (1998). *Electric Drives*, CRC Press,.

Casadei D., et al.,(2002). *FOC and DTC: Two viable schemes for induction motors torque control*, IEEE Trans. Power Electron., vol. 17, pp. 779–787, Sept..

Casadei D., et al., (2000*). Implementation of a Direct Torque Control Algorithm for Induction Motors Based on Discrete Space Vector Modulation*, IEEE Trans. Ind. Applicat., vol. 15, No.4 pp. 769–777, July.

Giuseppe S. et al. (2004). *Diret Torque Control of PWM Inverter-Fed AC Motors – A survey*, IEEE Trans. Ind. Applicat., vol. 51, pp. 744–757, Aug..

Koutsogiannis Z., et al., (2006). *Computer Analysis of a Direct Torque Control Induction Motor Drive Using a Fuzzy Logic Speed Controller,* XVII International Conference on Electrical Machines, Sept..

Brahmananda T. et al, (2006), *Sensorless Direct Torque Control of Induction Motor based on Hybrid Space Vector Pulsewidth Modulation to Reduce Ripples and Switching Losses – A Variable Structure Controller Approach*, IEEE Power India Conference, 10-12 Apr..

Chen L., et al., (2005). *A scheme of fuzzy direct torque control for induction machine*, IEEE Proceedings of the Fourth International Conference on Machine Learning and Cybernetics, Guangzhou, 18-21 Aug..

Mitronikas E. & Safacas A., (2004). *A Hybrid Sensorless Stator-Flux Oriented Control Method for Induction Motor Drive*, in 35th Annual IEEE Power Electronics Specialists Conference (PESC'04), June 20-25, , Aachen, Germany, pp. 3481-3485.

Grabowski P., (2000). *A Simple Direct Torque Neuro Fuzzy Control of PWM Inverter Fed Induction Motor Drive*, IEEE Trans. Ind. Electron., Vol. 47, No. 4, pp. 863-870, Aug..

Romeral L., et al. (2003). *Novel Direct Torque Control (DTC) Scheme With Fuzzy Adaptive Torque-Ripple Reduction*, IEEE Trans. Ind. Electron., vol.50, pp.487–492,Jun..

Ortega M., et al., (2005). *Direct Torque Control of Induction Motors using Fuzzy Logic with current limitation*, IEEE Industrial Electronics Society, IECON 2005. 32nd Annual Conference.

Mitronikas E. & Safacas A., (2001). *A New Stator Resistance Tuning Method for Stator-Flux-Oriented Vector-Controlled Induction Motor Drive*, IEEE Transaction on Industrial Electronics, Vol. 48, No. 6, December 2001, pp. 1148 – 1157.

Mitronikas E. & Safacas A., (2005) . *An improved Sensorless Vector Control Method for an Induction Motor Drive*, IEEE Transaction on Industrial Electronics, Vol. 52, No. 6, December, pp. 1660-1668.

Miloudi A., et.al., (2004). Simulation and Modelling of a Variable Gain PI Controller For Speed Control of a Direct Torque Neuro Fuzzy Controlled Induction Machine Drive, in: proceedings of 35th Annual IEEE Power Electronics Specialists Conference (PESC'04), June , pp. 3493-3498.

Koutsogiannis Z. &, Adamidis G., (2007). Direct Torque Control using Space Vector Modulation and dynamic performance of the drive via a Fuzzy logic controller for speed regulation, in: proceedings of EPE.

Reddy T. B., at. al. 2006). Sensorless Direct Torque Control of Induction Motor based on Hybrid Space Vector Pulsewidth Modulation to Reduce Ripples and Switching Losses – A Variable Structure Controller Approach, IEEE Power India Conference.

H. Zatocil H., 2008. Sensorless Control of AC Machines using High-Frequency Excitation, in 13th International Power Electronics and Motion Control Conference EPE-PEMC, Poznan, Poland.

Gadoue S. M. at. al., (2009). Artificial intelligence-based speed control of DTC induction motor drives-A comparative study, J. Electric Power Syst. Res. 79, p.p. 210–219.

R. Zaimeddine at. al., (2007). Enhanced Direct Torque Control Using a Three-Level Voltage Source Inverter, Asian Power Electronics Journal, Vol. 1, No. 1, Aug 2007.

Xavier del Toro, at. al, (2005), New DTC Control Scheme for Induction Motors fed with a Three-level Inverter, AUTOMATIKA 46(2005) 1-2, pp. 73–81

R. Zaimeddine, at. al., (2010) DTC Control Schemes for Induction Motorfed by Three-Level NPC-VSI Using Space Vector Modulation, SPEEDAM 2010 International Symposium on Power Electronics, Electrical Drives, Automation and Motion

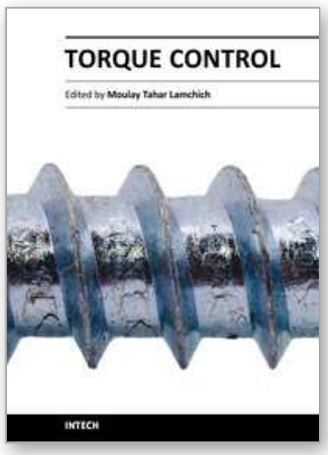

Torque Control
Edited by Prof. Moulay Tahar Lamchich

ISBN 978-953-307-428-3
Hard cover, 292 pages
Publisher InTech
Published online 10, February, 2011
Published in print edition February, 2011

This book is the result of inspirations and contributions from many researchers, a collection of 9 works, which are, in majority, focalised around the Direct Torque Control and may be comprised of three sections: different techniques for the control of asynchronous motors and double feed or double star induction machines, oriented approach of recent developments relating to the control of the Permanent Magnet Synchronous Motors, and special controller design and torque control of switched reluctance machine.

How to reference
In order to correctly reference this scholarly work, feel free to copy and paste the following:

Adamidis Georgios, and Zisis Koutsogiannis (2011). Direct Torque Control using Space Vector Modulation and Dynamic Performance of the Drive, via a Fuzzy Logic Controller for Speed Regulation, Torque Control, Prof. Moulay Tahar Lamchich (Ed.), ISBN: 978-953-307-428-3, InTech, Available from: http://www.intechopen.com/books/torque-control/direct-torque-control-using-space-vector-modulation-and-dynamic-performance-of-the-drive-via-a-fuzzy

INTECH
open science | open minds

InTech Europe
University Campus STeP Ri
Slavka Krautzeka 83/A
51000 Rijeka, Croatia
Phone: +385 (51) 770 447
Fax: +385 (51) 686 166
www.intechopen.com

InTech China
Unit 405, Office Block, Hotel Equatorial Shanghai
No.65, Yan An Road (West), Shanghai, 200040, China
中国上海市延安西路65号上海国际贵都大饭店办公楼405单元
Phone: +86-21-62489820
Fax: +86-21-62489821

IntechOpen